AFOSR-TR- 87-0419

February 1987

University of Virginia

STRUCTURE AND DYNAMICS OF EXCITED ATOMS

Annual Technical Report
Grant No. AFOSR-85-0016

by

T. F. Gallagher

Prepared for:

AIR FORCE OFFICE OF SCIENTIFIC RESEARCH
Building 410
Bolling Air Force Base
Washington, DC 20332

Attn.: Dr. Ralph Kelley
General Physics Division
Directorate of Physics

Thomas F. Gallagher
Principal Investigator

UNCLASSIFIED
SECURITY CLASSIFICATION OF THIS PAGE

AD-A179887

REPORT DOCUMENTATION PAGE

1a. REPORT SECURITY CLASSIFICATION UNCLASSIFIED	1b. RESTRICTIVE MARKINGS
2a. SECURITY CLASSIFICATION AUTHORITY	3. DISTRIBUTION/AVAILABILITY OF REPORT Approved for public release; Distribution unlimited
2b. DECLASSIFICATION/DOWNGRADING SCHEDULE	
4. PERFORMING ORGANIZATION REPORT NUMBER(S)	5. MONITORING ORGANIZATION REPORT NUMBER(S) AFOSR-TR- 87-0419
6a. NAME OF PERFORMING ORGANIZATION University of Virginia 6b. OFFICE SYMBOL (If applicable)	7a. NAME OF MONITORING ORGANIZATION AFOSR/NP
6c. ADDRESS (City, State, and ZIP Code) Department of Physics Charlottsville, VA 22901	7b. ADDRESS (City, State, and ZIP Code) Building 410 Bolling AFB DC 20332-6448
8a. NAME OF FUNDING/SPONSORING ORGANIZATION Same as 7a 8b. OFFICE SYMBOL (If applicable) NP	9. PROCUREMENT INSTRUMENT IDENTIFICATION NUMBER AFOSR 85-0016
8c. ADDRESS (City, State, and ZIP Code) Same as 7b	10. SOURCE OF FUNDING NUMBERS PROGRAM ELEMENT NO. 61102F; PROJECT NO. 2301; TASK NO. A4; WORK UNIT ACCESSION NO.
11. TITLE (Include Security Classification) "Structure and Dynamics of Excited Atoms" (U)	
12. PERSONAL AUTHOR(S) Thomas F. Gallagher	
13a. TYPE OF REPORT FINAL 13b. TIME COVERED FROM 1 Nov 84 TO 31 Oct 86	14. DATE OF REPORT (Year, Month, Day) February 1987 15. PAGE COUNT 52
16. SUPPLEMENTARY NOTATION	
17. COSATI CODES FIELD / GROUP / SUB-GROUP	18. SUBJECT TERMS (Continue on reverse if necessary and identify by block number) Radiation, Collisions, Multiphoton

19. ABSTRACT (Continue on reverse if necessary and identify by block number)

Research has been conducted on the interactions of single atoms and colliding pairs of atoms with strong radiation fields by making quantative measurements of multiphoton processes involving highly excited atoms in microwave fields. Among the results of the research have been the discovery that blackbody radiation can be used to measure avoided crossings of energy levels in an electric field, and the first measurements of microwave multiphoton resonances. Resonant collisions of K atoms have also been studied and very narrow collisional resonances have been observed.

20. DISTRIBUTION/AVAILABILITY OF ABSTRACT ☒ UNCLASSIFIED/UNLIMITED ☐ SAME AS RPT. ☐ DTIC USERS	21. ABSTRACT SECURITY CLASSIFICATION Unclassified
22a. NAME OF RESPONSIBLE INDIVIDUAL Dr Ralph E. Kelley	22b. TELEPHONE (Include Area Code) 202, 767-4908 22c. OFFICE SYMBOL NP

DD FORM 1473, 84 MAR 83 APR edition may be used until exhausted. All other editions are obsolete.

SECURITY CLASSIFICATION OF THIS PAGE
UNCLASSIFIED

I. Introduction

The objective of this research is to investigate how single atoms and colliding pairs of atoms interact with strong radiation fields. Our approach is to make quantitative measurements of multiphoton processes involving highly excited atoms in microwave fields. These measurements serve to guide our thinking toward the most productive theoretical points of view.

II. Research accomplishments during the period 1 November 1985-31 October 1986

During this period we have worked on several projects which are outlined briefly below.

Anticrossing Spectroscopy

In the previous year we discovered the fact that blackbody radiation could be used to measure avoided crossings of energy levels in an electric field, and the first report of this was published in Physical Review Letters during the period covered by this report. It is included here as Appendix A. During the period covered by this report we refined the measurement technique, improving the precision by an order of magnitude, and worked out the theory in detail. These more comprehensive results were published in Physical Review A. A copy of this article is included as Appendix B.

Ionization by Quasistatic and Microwave Fields

A paper describing the electric field ionization of Na states down to n=8 was submitted for publication and is included as Appendix C. The observed results are consistent with extrapolations from higher n states. Prior to this work no one had observed such low lying states by field ionization, so it was not *a priori* obvious that this would be the case.

We have now made microwave ionization measurements for Na at frequencies of 4, 2, and 0.6 GHz, and all the data exhibit the $1/3n^5$ dependence observed at 15 GHz and 8 GHz. We plan to do an experiment at a frequency of about 100 MHz before publishing this work.

Microwave Multiphoton Transitions

During this period we have made the first measurements of microwave multiphoton resonances, observing up to 29 photon transitions. These observations strongly suggest that the best way to think about this problem is from the point of view of the so-called "dressed" states in which the effect of the external field is accounted for on an equal footing. A report of this work has been accepted for publication in Physical Review Letters and is included here as Appendix D. This work and the related analysis are also reported in the proceedings of a workshop on atoms in Strong fields, and this is included as Appendix E.

Resonant Collisions

During this year we have also worked on resonant collisions of K atoms. Primarily we have concentrated on the production of velocity selected beams, and using this approach we have seen very narrow collisional resonances.

Anticrossing Spectroscopy of Rydberg Atoms Using Blackbody Radiation

R. C. Stoneman and T. F. Gallagher

Department of Physics, University of Virginia, Charlottesville, Virginia 22901

(Received 24 July 1985)

We report the observation of anticrossing signals arising from the interaction of 300-K blackbody radiation with Rydberg atoms near avoided crossings of Stark levels. The role of the blackbody radiation is roughly analogous to that of the resonance fluorescence in traditional anticrossing spectroscopy. We present preliminary results for avoided crossings of ns states with $n-2$ Stark states in potassium for n in the range 18–21.

PACS numbers: 31.60.+b, 32.60.+i

Level crossing and anticrossing spectroscopy is by now a classic method for obtaining information about the details of excited atomic energy levels.[1,2] For example, fine and hyperfine structure, Stark and Zeeman shifts, oscillator strengths, and lifetimes have been obtained in this fashion.[3] Although the level crossings or anticrossings are not usually thought of as being of physical interest themselves, in dynamical situations such as collisions[4] or strong time-varying fields they are the determining factor.[5,6] For example, recent microwave-ionization experiments have shown that a state of principal quantum number n can be ionized by a microwave electric field of amplitude $1/3n^5$, the field at which the highest-energy n and lowest-energy $n+1$ Stark states would cross in the absence of any coupling.[7,8] The existence of a coupling V leads to an avoided crossing of magnitude $2V$, and permits the transition from n to $n+1$. This transition, which is the rate-limiting step in microwave ionization, occurs when the microwave frequency $f \sim 2V$.[7]

Direct measurements of avoided crossings would clearly be desirable, and this is easily done by conventional laser spectroscopy if the avoided crossings are large enough (~ 1 cm^{-1}). For many cases of interest, however, the avoided crossings are small, < 2 GHz, and other techniques, such as anticrossing spectroscopy and radio-frequency spectroscopy,[9] become more attractive. Of these, anticrossing spectroscopy is the more straightforward.[2]

Here we report a novel form of anticrossing spectroscopy using the 300-K blackbody radiation.[10,11] To our knowledge, this is the first use of the 300-K blackbody radiation, which is usually an experimental nuisance, to do high-resolution spectroscopy. In particular we describe preliminary observations of the anticrossings between the ns states and lowest-energy $n-2$ Stark states in potassium.

The experiment is easily understood with use of the $19s$ state as an example. In Fig. 1 we show the relevant energy levels and their electric-field dependences. Only the extreme upper and lower members of the manifold of $n=17$ Stark states are shown. At the fields of interest, ~ 550 V/cm, each $n=17$ Stark state is a linear combination of primarily the zero-field $n=17$, $l \geq 3$ states. At a field of 550 V/cm the $19s$ state crosses the lowest energy $|m_l|=0$ and 1 Stark states. Here m_l and m_j are the orbital and total azimuthal angular-momentum quantum numbers. The $|m_l|$ Stark levels are unresolved in Fig. 1 itself, but in the inset we show an expanded view of the avoided crossings. The $19s$ and the lowest-energy $|m_l|=0$ and 1 Stark states, with the assumption of no interaction, are shown by broken lines. Adding the interactions V_0 and V_1 (the subscripts denote the $|m_l|$ of the Stark state), originating from the large quantum defects of

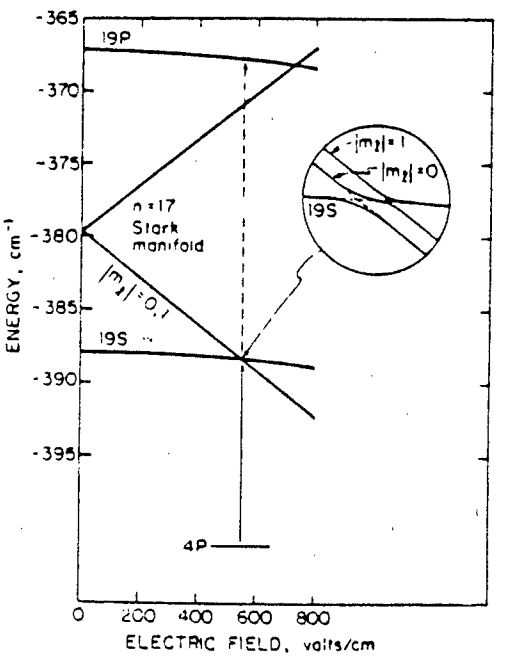

FIG. 1. K level diagram showing the intersection of the $19s$ state with the lowest-energy $n=17$, $|m_l|=0$ and 1 Stark states. The laser excitation from the $4p$ state is shown by the solid arrow, and the blackbody excitation to the $19p$ state is shown by the dashed arrow. The inset is an expanded view of the avoided crossing of the $|m_l|=\frac{1}{1}$ states. The $19s$ and the $|m_l|=0$ and 1 states with no interaction are shown by broken lines; the real states which occur with the interaction are shown as solid lines.

the low-l states and the p-state spin-orbit interaction, respectively, results in the real $|m_j| = \frac{1}{2}$ levels shown by the solid lines which have avoided crossings of $2V_0$ and $2V_1$. If we follow the lowest-energy real level through the first crossing, it smoothly changes from being purely s in character to a pure $|m_l| = 0$ Stark state (it is at all times $|m_j| = \frac{1}{2}$). At the point of the crossing it is a 50-50 mixture of the two. Similarly, the middle real level changes from a pure $|m_l| = 0$ Stark state to pure $19s$ as the crossing is traversed. Analogous statements apply to the second crossing.

Let us now consider the effect of the avoided crossing on our experiment. Potassium atoms in a thermal beam pass between two electric-field plates 1.07(1) cm apart where they are excited in a static field by two 5-ns dye-laser pulses from the ground state $4s$ to the $4p$ state and then to the levels in the vicinity of the level crossings of Fig. 1. For a period of 3 μs immediately following the laser pulses, the atoms are exposed to the 300-K blackbody radiation which further excites roughly 10% of the atoms to higher-lying states. After this 3 μs period the atoms are field ionized and detected by a particle multiplier, the output of which is recorded with a gated integrator. The field ionization is done in such a manner that only the signal corresponding to the $19p$ state is recorded. In our experiment the laser bandwidth is broad enough, $\sim \frac{1}{2}$ cm^{-1}, to encompass all states of interest in the vicinity of the crossing of Fig. 1. If we assume for a moment that the Stark states are composed not primarily of, but only of, $l \geq 3$ states, then a pure Stark state cannot be excited from the $4p$ state, nor can it be driven by blackbody radiation to the $19p$ state. Thus one of the real states of Fig. 1 can be excited by the laser from the $4p$ state only to the extent that it contains $19s$ character, and only the $19s$ character can lead to a subsequent blackbody-radiation–induced transition to the $19p$ state.

Now consider what happens when the static field is swept through the first avoided crossing of the inset of Fig. 1. Below the avoided crossing the only excitation by the laser is to the $19s$ state, the lowest real level of Fig. 1, and N atoms are excited to the $19s$ state. A fraction γ of these atoms is transferred to the $19p$ state by blackbody radiation, leading to $N\gamma$ $19p$ atoms which are detected. At the avoided crossing the two lowest real states of the inset of Fig. 1 are both 50-50 mixtures of $19s$ and $n = 17$ Stark states. Thus $N/2$ atoms are excited to each real state, while the total number of atoms excited by the laser is still N. However, as each of these states is only half $19s$, the fraction of atoms undergoing blackbody-radiation transitions to the $19p$ state is only $\gamma/2$, and the number of $19p$ atoms produced is only $N\gamma/2$. At a field above the avoided crossing the $19s$ character resides entirely in the middle real level of the inset of Fig. 1. Thus N atoms are excited to this level and a fraction γ transferred to the $19p$ level, resulting in $N\gamma$ $19p$ atoms. In other words, as the static field is swept through the avoided crossing, the number of $19p$ atoms detected drops by half and then returns to its original value. In fact, there is a dramatic decrease in the number of $19p$ atoms observed as the field is swept through the avoided crossings as shown by Fig. 2.

In practice our observed signal does not exhibit a 50% decrease because of the fact that the $n = 17$ Stark state is not composed only of $l \geq 3$ states. By taking excitation spectra from the $4p$ state, we found that the total oscillator strength to the $|m_l| = 0$ and 1 Stark states is 12(2)% of the oscillator strength to the $19s$ state. Similarly, we recorded spectra for excitation from the $4p$ state with subsequent blackbody-radiation excitation to the $19p$ state. These spectra together with the previous excitation spectra allowed us to determine that the blackbody-radiation transition rate to the $19p$ state from the $n = 17$ Stark state is 16(4)% of the rate from the $19s$ state. Thus the model used above, based on pure $l \geq 3$ composition of the Stark states, is only approximately correct.

There are two systematic checks which we performed in the course of this work. First, the $19p$ signal was identified as arising from blackbody-radiation excitation in the usual way[10]: The $19p$ signal is zero for no delay between laser excitation and field ionization, grows monotonically with increasing delay, and saturates at delays of ~ 7 μs. Second, in principle the

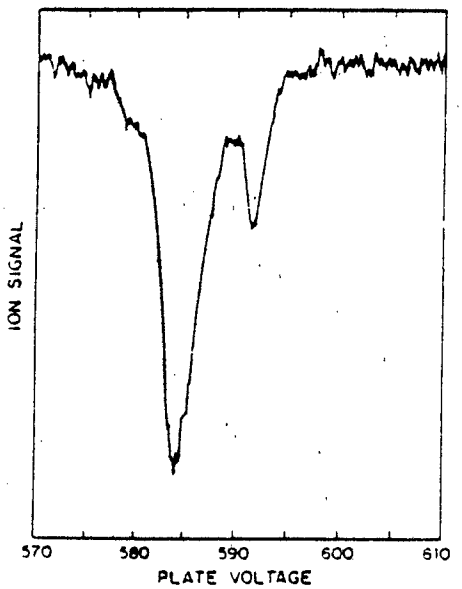

FIG. 2. Anticrossing signal from the avoided crossings of the $19s$ state with the lowest $n = 17$ Stark states corresponding to Fig. 1. The signal is obtained by observation of the $19p$ state population as the static field is swept.

TABLE I. Observed anticrossings.

State	$\lvert m_l\rvert = 0$ Position[a] (V/cm)	$\lvert m_l\rvert = 0$ Width (FWHM) (V/cm)	$\lvert m_l\rvert = 1$ Position[a] (V/cm)	$\lvert m_l\rvert = 1$ Width (FWHM) (V/cm)
18*s*	753.0(3)	5.8(6)	762.8(5)	3.5(10)
19*s*	546.1(2)	4.1(2)	552.9(2)	2.0(3)
20*s*	404.0(2)	2.8(6)	409.0(3)	1.4(2)
21*s*	304.7(2)	1.9(3)	308.3(2)	1.1(4)

[a]The 1% field-calibration uncertainty is not included.

number of atoms excited by the laser is invariant as the static field is swept through the avoided crossing, and in practice we were unable to observe any variation.

Our anticrossing signals are obtained under conditions which are significantly different from those of previous anticrossing experiments. We detect atomic populations produced by isotropic blackbody radiation, whereas in most previous experiments the signals were detected by observation of resonance fluorescence of specified polarization in a specified direction. (A notable exception is the series of optogalvanic experiments of Hannaford and Series,[12] which relied at least partially upon a nonlinear effect.) Our laser excitation is pulsed, while in the previous anticrossing experiments the excitation and fluorescence were in the steady state. Finally, in most previous experiments the avoided crossings were of the same order of magnitude as the decay rates Γ; in our case $V >> \Gamma$.

These differences preclude the use of the steady-state anticrossing treatments,[13] and we have thus derived the solution appropriate to our pulsed experiment.[14] For the case in which the exposure time of the atoms to the blackbody radiation is short compared to the inverse of the difference of the decay rates of the *ns* and $n-2$ Stark states, the solution takes a simple form. The anticrossing signal has both Lorentzian and dispersion components which have the same centers and equal widths. The relative strengths and signs of these two components depend on the dipole matrix elements connecting the *ns* and $n-2$ Stark states to the 4*p* and *np* states.

In fact, the above decay- versus exposure-time condition is well satisfied in our experiment. The exposure time is 3 μs, and the decay times of the 19*s* and $n=17$ Stark states are 9(2) and 7(2) μs, respectively. Furthermore, if the dominant laser excitation from the 4*p* state is to the *ns* state and the dominant blackbody-radiation excitation to the *np* state is from the *ns* state, the Lorentzian component is dominant; this condition holds in our experiment. This, coupled with the fact that there is no obvious dispersion in our data, led us to simply fit our data with a Lorentzian lineshape. The results of these fits for the signals arising from the crossings of the *ns* and $n-2$ Stark states for n in the range 18–21 are given in Table I.

The reproducibility of the positions of the anticrossing signals is substantially better than our ability to measure the spacing of our present field plates. To show the reproducibility, we give the uncertainties in Table I assuming that the plate separation is perfectly known, and as noted in Table I, a 1% calibration error must be added. The field positions scale as $n^{-5.25}$, which is reasonably close to the n^{-5} dependence expected for Stark shifts scaling as n^2 and energy spacings scaling as n^{-3}. For comparison we give in Table II the theoretical positions and widths which are obtained by diagonalization of the energy matrix.[15] The

TABLE II. Calculated positions and widths and corrected experimental widths.

State	$\lvert m_l\rvert = 0$ Calculated Position (V/cm)	$\lvert m_l\rvert = 0$ Calculated Width (GHz)	$\lvert m_l\rvert = 0$ Experimental corrected width (GHz)	$\lvert m_l\rvert = 1$ Calculated Position (V/cm)	$\lvert m_l\rvert = 1$ Calculated Width (MHz)
18*s*	753.80	0.93	0.90(20)	763.85	80
19*s*	546.40	0.64	0.76(12)	553.44	61
20*s*	404.13	0.45	0.58(10)	409.17	47
21*s*	304.14	0.32	0.40(8)	307.87	39

experimental crossing positions of Table I are in excellent agreement with these calculations.

From our point of view the widths of the avoided crossing signals are more interesting than the positions. To compare the calculated frequency widths of Table II with the observed field widths requires the conversion factors for the $18s$–$21s$ states, which are, respectively, 356, 403, 450, and 506 MHz/V·cm^{-1}. First, we note that the $|m_l|=1$ experimental widths are far larger than the calculated widths. Thus they are a measure of the field inhomogeneity ΔE, and using them, we find $\Delta E = 3.7\times10^{-3}E$, a value consistent with the mechanical tolerances of the plates. Subtraction of this instrumental width in quadrature from the observed $|m_l|=0$ widths of Table I gives the corrected $|m_l|=0$ widths of Table II, which are in reasonable agreement with the calculated values. The corrected experimental and calculated $|m_l|=0$ widths scale as $(n-\delta_s)^{-6}$, where δ_s is the s-state quantum defect.

The fact that we can observe the $|m_l|=1$ crossings at all underscores the importance of spin-orbit coupling for dynamic processes involving the Stark states. Previously, it was suggested that the differences in the field ionization of K and Na were due to the large K spin-orbit interaction.[16] On the basis of these measurements we estimate that the magnitude of the $|m_l|=1$ avoided crossings is ~ 100 MHz at $n=20$, a value which would be likely to cause nonadiabatic transitions with commonly used field-ionization slew rates.

More generally, this approach appears to be a simple yet powerful technique for the study of level crossings in atomic Rydberg states. After some refinements and more systematic tests, which are under way,[14] the method should be applicable to a variety of problems, such as the crossings of the extreme members of adjacent Stark manifolds which are crucial to microwave ionization.[7]

It is a pleasure to acknowledge useful discussions with D. J. Larson, W. E. Cooke, G. Janik, O. C. Mullins, and L. A. Bloomfield. This work was supported by the U. S. Air Force Office of Scientific Research under Grant No. AFOSR-85-0016.

[1]F. D. Colegrove, P. A. Franken, R. R. Lewis, and R. H. Sands, Phys. Rev. Lett. 3, 420 (1959).

[2]T. G. Eck, L. L. Foldy, and H. Weider, Phys. Rev. Lett. 10, 239 (1963).

[3]W. Happer and R. Gupta, in *Progress in Atomic Spectroscopy*, edited by W. Hanle and H. Kleinpoppen (Plenum, New York 1978); H. J. Beyer and H. Kleinpoppen, *ibid.*

[4]L. D. Landau and E. M. Lifshitz, *Quantum Mechanics, Nonrelativistic Theory* (Pergamon, New York, 1965).

[5]T. F. Gallagher, L. M. Humphrey, W. E. Cooke, R. M. Hill, and S. A. Edelstein, Phys. Rev. A 16, 1098 (1977).

[6]T. H. Jeys, G. W. Foltz, K. A. Smith, E. J. Beiting, F. G. Kellert, F. B. Dunning, and R. F. Stebbings, Phys. Rev. Lett. 44, 390 (1980).

[7]P. Pillet, W. W. Smith, R. Kachru, N. H. Tran, and T. F. Gallagher, Phys. Rev. Lett. 50, 1042 (1983).

[8]D. R. Mariani, W. Van de Water, P. M. Koch, and T. Bergeman, Phys. Rev. Lett. 50, 1261 (1983).

[9]J. R. Rubbmark, M. M. Kash, M. G. Littman, and D. Kleppner, Phys. Rev. A 23, 3107 (1981).

[10]T. F. Gallagher and W. E. Cooke, Phys. Rev. Lett. 42, 835 (1979).

[11]E. J. Beiting, G. F. Hildebrandt, F. G. Kellert, G. W. Foltz, K. A. Smith, F. B. Dunning, and R. F. Stebbings, J. Chem. Phys. 70, 3551 (1979).

[12]P. Hannaford and G. W. Series, Phys. Rev. Lett. 48, 1326 (1982).

[13]H. Weider and T. G. Eck, Phys. Rev. 153, 103 (1967).

[14]R. C. Stoneman, G. Janik, and T. F. Gallagher, to be published.

[15]M. L. Zimmerman, M. G. Littman, M. M. Kash, and D. Kleppner, Phys. Rev. A 20, 2251 (1979).

[16]T. F. Gallagher and W. E. Cooke, Phys. Rev. A 19, 694 (1979).

Anticrossing spectroscopy of K Rydberg atoms using 300-K blackbody radiation

R. C. Stoneman, G. Janik, and T. F. Gallagher
Department of Physics, University of Virginia, Charlottesville, Virginia 22901
(Received 31 March 1986)

The avoided crossings in an electric field of K s and p states with the nearly hydrogenic Stark manifold states have been investigated using 300-K blackbody radiation. Anticrossings between states of the same $|m_l|$ for which the $|m_l|$ values are the same or differ by one are encountered. The anticrossings between states of the same $|m_l|$ are quite wide as they are due to core penetration and polarization effects. The anticrossings for which $|m_l|$ differs by one are produced by the spin-orbit interaction and are accordingly quite small. We present results for the ns states for n in the range 18–29 and for the np states for n in the range 19–23.

I. INTRODUCTION

Level crossing[1] and anticrossing[2] spectroscopy, techniques based on the crossing or near crossing of atomic energy levels in an external field, have been widely used in the past to measure properties of atomic excited states. Specifically these techniques have yielded measurements of fine and hyperfine structure, Stark and Zeeman shifts, oscillator strengths, and lifetimes.[3–5] In addition to being a useful artifact, the avoided crossings in an electric field have recently been recognized as intrinsically important factors in static[6] and dynamic[7] field ionization of Rydberg atoms.

The electric-field-induced avoided crossings of Rydberg-atom energy levels have previously been directly measured by laser spectroscopy.[3] However, this technique is limited to levels which do not approach each other more closely than the laser linewidth. For typical pulsed lasers this limit is about 5 GHz. For avoided crossings narrower than this, rf spectroscopy has been used to accurately measure the separation at the avoided crossing.[6] The rf technique, however, has the limitation that one of the levels must be preferentially excited and one preferentially detected. These conditions are not met for all avoided crossings. Also, the rf technique is inherently two dimensional, requiring rf scans to be taken at several electric field values in order to find the point of closest approach.

We elaborate here on our earlier report[9] of a new method of anticrossing spectroscopy using 300-K blackbody radiation. The technique is straightforward and yields good results even for those situations where the rf technique is least sensitive. In this report we develop the theory of the anticrossing signals that we observe, and present new data with improved resolution. We also describe our investigations of other techniques for observing anticrossing signals which are, in principle, attractive. As we shall see these alternatives are not as useful as the blackbody-radiation method.

II. THEORY

As two Stark-shifted atomic levels approach each other with a change in the electric field, any perturbation which couples the levels will cause them to repel. In hydrogen there is no perturbation save the negligibly small spin-orbit interaction and the levels cross, for all practical purposes. In the alkali metals the interaction of the valence electron with the ion core introduces a perturbation between atomic levels with the same value of $|m_l|$. The dotted lines of Fig. 1 show two levels $|a\rangle$ and $|b\rangle$ which cross when the perturbation between them is ignored. When the perturbation V is included we obtain the real eigenstates $|u\rangle$ and $|l\rangle$ (solid curves in Fig. 1). The eigenstates are superpositions of the unperturbed states and consist of 50-50 mixtures at the point of closest approach. At a specific electric field the energies of states $|a\rangle$ and $|b\rangle$ are given by the complex energies W_a and W_b which are given by

$$W_a = E_a - i\Gamma/2 , \tag{1}$$

$$W_b = E_b - i\Gamma/2 , \tag{2}$$

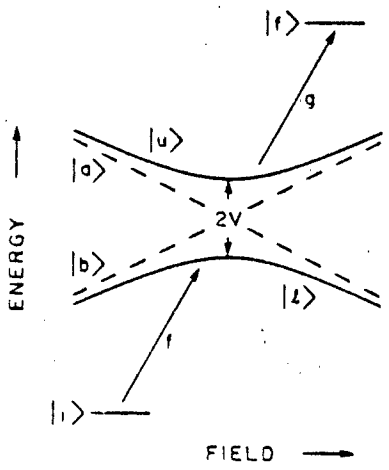

FIG. 1. Stark states $|a\rangle$ and $|b\rangle$ cross when the perturbation between them is ignored. The real states $|u\rangle$ and $|l\rangle$ result from the perturbation V. In our experiment the initial state $|i\rangle$ is the $4p$ state of potassium. The laser excitation is represented by f, and the blackbody excitation by g.

The imaginary parts of W_a and W_b allow for the radiative decay of these levels at a rate Γ. For simplicity we have assumed Γ to be the same for $|a\rangle$ and $|b\rangle$. If the off-diagonal matrix element coupling $|a\rangle$ and $|b\rangle$ is given by V the superposition can be parameterized in the following way:

$$|u\rangle=(\cos\theta)|a\rangle+(\sin\theta)|b\rangle\ , \tag{3}$$

$$|l\rangle=(-\sin\theta)|a\rangle+(\cos\theta)|b\rangle\ , \tag{4}$$

where

$$\tan(2\theta)=\frac{2V}{E_a-E_b},\quad 0\le\theta\le\pi/2\ . \tag{5}$$

In our experiment we excite the eigenstates with a pulsed dye laser. The laser linewidth is about 0.5 cm^{-1}, which is much larger than the closest approach of the eigenstates we have investigated (<1 GHz). This means that we excite both eigenstates when the field is near the avoided crossing. The pulse width of the laser is about 5 ns which implies a coherent bandwidth of roughly 100 MHz. If the states are separated by more than this amount we excite an incoherent mixture; if the spacing is less, we excite a coherent superposition. We shall show that with our technique, the same type of signal is obtained in either case so we shall consider explicitly the case of incoherent excitation. The radiative decay times, $1/\Gamma$, of these eigenstates are generally greater than 5 μs. Part, ~10%, of this observed decay rate is due to excitation by the ambient 300-K blackbody radiation to higher excited states.[10] The anticrossing signals that we observe are a result of the interaction between the blackbody radiation and the eigenstates $|u\rangle$ and $|l\rangle$ near the avoided crossing.

As a model for our anticrossing signal we assume the following sequence of events. First a coherent or incoherent mixture of eigenstates is produced at a fixed dc electric field. This excitation is assumed to occur instantaneously at time $t=0$. Then the mixture of states evolves in time under the influence of the static atomic Hamiltonian and dc field. During this time these states are driven by blackbody radiation to a higher-lying atomic state which is assumed not to decay. Finally, at time $t=T$ the atoms in the higher excited state are selectively field ionized and detected.

To calculate the probability of an atom reaching the final state $|f\rangle$ we first calculate the probabilities P_u and P_l of reaching states $|u\rangle$ and $|l\rangle$. If f_a and f_b are the dipole matrix elements for excitation by the laser field E_L from the initial state $|i\rangle$ to states $|a\rangle$ and $|b\rangle$, i.e., $f_a=\langle a|\mu E_L|i\rangle$ and $f_b=\langle b|\mu E_L|i\rangle$ then P_u and P_l are given by

$$P_u=|\langle u|\mu E_L|i\rangle|^2=(f_a\cos\theta+f_b\sin\theta)^2\ ,$$
$$P_l=|\langle l|\mu E_L|i\rangle|^2=(f_b\cos\theta-f_a\sin\theta)^2\ . \tag{6}$$

If we take the ratio f of these matrix elements, $f=f_b/f_a$, then Eq. (6) may be written

$$P_u=(\cos\theta+f\sin\theta)^2/(1+f^2)\ ,$$
$$P_l=(f\cos\theta-\sin\theta)^2/(1+f^2)\ . \tag{7}$$

We note that $P_u+P_l=1$, independent of θ. In other words the total number of atoms excited to the pair of states u and l by the laser is independent of the field.

The probability of atom's having been driven to the final state $|f\rangle$ by a time T is given by

$$P(T)=\int_0^T(P_u g_u^2+P_l g_l^2)e^{-\Gamma t}dt\ , \tag{8}$$

where $g_u=\langle f|\mu E_B|u\rangle$ and $g_l=\langle f|\mu E_B|l\rangle$ are the blackbody-radiation matrix elements connecting the $|u\rangle$ and $|l\rangle$ states to the $|f\rangle$ state. Expressing g_u and g_l in terms of the analogous matrix elements from the $|a\rangle$ and $|b\rangle$ states which are $g_a=\langle f|\mu E_B|a\rangle$ and $g_b=\langle f|\mu E_B|b\rangle$ leads to

$$g_u^2=(g_a\cos\theta+g_a\sin\theta)^2\ ,$$
$$g_l^2=(g_b\cos\theta-g_a\sin\theta)^2\ . \tag{9}$$

Introducing the ratio of the matrix elements $g=g_b/g_a$ leads to

$$g_u^2=(\cos\theta+g\sin\theta)/(1+g^2)\ ,$$
$$g_l^2=(g\cos\theta-\sin\theta)/(1+g^2)\ . \tag{10}$$

Substituting into Eq. (8) the expressions of Eqs. (10) and (7) yields:

$$P(T)=\left[\frac{(\cos\theta+f\sin\theta)^2(\cos\theta+g\sin\theta)^2}{(1+f^2)(1+g^2)}+\frac{(f\cos\theta-\sin\theta)(g\cos\theta-\sin\theta)}{(1+f^2)(1+g^2)}\right]\times\frac{1-e^{-\Gamma T}}{\Gamma}\ . \tag{11}$$

If we now replace $\cos\theta$ and $\sin\theta$ using Eq. (5) we can rewrite Eq. (11) as

$$P(T)=\left[(1+f^2g^2)+\left[\frac{(2V)^2}{(2V)^2+(E_a-E_b)^2}\right]\left[2fg-\frac{(f^2-1)(g^2-1)}{2}\right]+\left[\frac{(2V)(E_a-E_b)}{(2V)^2+(E_a-E_b)^2}\right][-f(g^2-1)-g(f^2-1)]\right]\left[\frac{1-e^{-\Gamma T}}{\Gamma}\right]\ . \tag{12}$$

All the line-shape dependence is contained in the large square brackets of Eq. (12). To a good approximation f and g are constant and the unperturbed energies E_a and E_b have linear Stark shifts in the small region near an avoided crossing. In this approximation the first term in the brackets of Eq. (12) is a constant, the second a Lorentzian, and the third a dispersion curve. The Lorentzian and dispersion curves have equal centers and widths.

Although the anticrossing signal depends in a complicated way on both f and g several cases are fairly simple. If $f=g=1$ the signal is a pure Lorentzian with amplitude equal to the dc component. If $f=g=0$ the signal is a pure Lorentzian with amplitude $-\frac{1}{2}$ times the dc component. For some of the avoided crossings we investigated (the s-level anticrossings) the f and g values were determined to be ~ 3 by laser measurements away from the avoided crossings. This results in signals which have both Lorentzian and dispersion components.

Let us return for a moment to our earlier assertion that in our experiments, even if the separation of the $|u\rangle$ and $|l\rangle$ states is small enough that these states may be excited coherently, we would be unlikely to observe the coherence. It should be manifested as beats at the angular frequency ω_{u-l} corresponding to the $u-l$ energy spacing. First, as shown by Eq. (8) our signal is an integral, so that even if there was a modulation of depth δ in P_u and P_l the depth of modulation would be reduced to $\delta\Gamma/\omega_{u-l}$ in the physically meaningful case $\Gamma \ll \omega_{u-l}$. For a 50-MHz-wide avoided crossing and $1/\Gamma = 5$ μs the ratio Γ/ω_{u-l} is 0.67×10^{-3}. It is unlikely that we would be able to detect a quantum beat modulation, usually not large to begin with,[11] after such a reduction. Second, our field ionization detector has a rise time of ~ 0.5 μs limiting observable beat frequencies to < 1 MHz, which is below the detectable limit for our field inhomogeneity. Finally, we saw no dependence of the observed signals on delay time before applying the ionizing pulse. Thus we are confident that our earlier restriction to the case of incoherent excitation of the $|u\rangle$ and $|l\rangle$ states is adequate for the description of our problem.

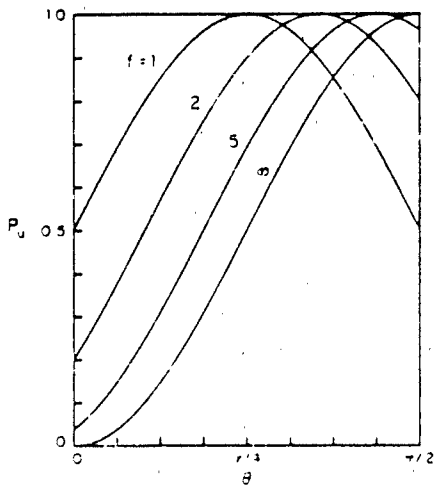

FIG. 2. Normalized probability for excitation to the real upper state ($|u\rangle$), as a function of the crossing parameter θ. P_u is shown for several positive values of $f=f_b/f_a$. For negative f, $P_u(\theta,-f)=1-P_u(\pi/2-\theta,f)$. For the lower state ($|l\rangle$), $P_l=1-P_u$.

At this point it is interesting to digress for a moment to consider the alternative approach of using rf spectroscopy in conjunction with the same broadband exciting laser. The excitation probability P_u is plotted in Fig. 2 for several values of f. For $f=1$ the two eigenstates have equal excitation probability away from the avoided crossing. At the point of closest approach, $\theta=\pi/4$, the excitation is all directed into the $|u\rangle$ state. If an rf field is applied with frequency $\nu=2$ V/h the level populations will equalize and a sharp increase (decrease) of the field ionization of the $|l\rangle$ ($|u\rangle$) state will occur. This situation is most favorable for the rf measurement technique. As f increases, the relative excitation probability P_u/P_l at the point of closest approach decreases until at very large f values $P_u=P_l$. The rf technique is therefore very insensitive for large values of f.

III. EXPERIMENTAL PROCEDURE

Observation of the anticrossing signals described here requires an experimental arrangement very similar to that used in previous field ionization studies.[12] A beam of potassium atoms passes between two electric field plates 1.590(1) cm apart. The atoms are stepwise excited by two pulsed dye lasers, from the $4s$ the $4p_{1/2}$ or $4p_{3/2}$ state with the "red" laser, and then from the $4p$ to the desired Rydberg state with the "blue" laser. The lasers are linearly polarized either parallel or perpendicular to the electric field, depending on the state desired. A dc voltage is applied to the plates, exposing the atoms to a uniform electric field. Approximately 3 μs after the laser pulses, a high-voltage pulse with a rise time 300 ns is applied to the plates. The Rydberg atoms are field ionized by this pulse, and the ions are extracted through small holes in the upper field plate, where they are detected by a particle multiplier. The output from the multiplier is fed to two gated integrators which provide temporal resolution of the field ionization signal.

To record an anticrossing signal, the dc field is swept while all other parameters remain fixed. The integrator gates are centered on two different features of the time-resolved field ionization signal. One feature changes with the dc field and represents the signal, while the other feature remains constant and is used to normalize the signal with respect to laser power fluctuations. The red laser is run with enough power to saturate the $4s$ to $4p$ transition in order to reduce the noise.

The blackbody excited atoms are easy to distinguish from those which are excited only by the laser. First, because the blackbody excited atoms lie in higher states than the directly excited atoms, they ionize at a lower field and hence at an earlier time. Second, since the blackbody radiation is present at all times, a signal induced by it increases as T (the field ionization pulse delay) increases; the signal from the directly excited atoms decreases as T increases. The blackbody signal eventually decreases for large delays and the approximately 3 μs delay used was the value which gave the maximum signal. There was no observed dependence of the line shape on Γ.

A more difficult problem was the selection of the features of the time-resolved field ionization signal on which to set the gates of the integrators. The field ionization spectrum of potassium is fairly rich because the wide variety of avoided crossings encountered by each state on its path to field ionization results in a combination of diabatic and adiabatic traverses which increases the complexity of the field ionization signal.[12] In addition there are generally several states excited by the blackbody radiation. Nevertheless, it is possible by visually observing an oscilloscope signal while scanning the dc voltage through the avoided crossing to pick out features of the field ionization signal which change significantly in amplitude. This becomes more difficult for the extremely narrow crossings and it is sometimes necessary to calculate their positions by scaling from previously measured values for similar but wider crossings of lower principle quantum number n.

IV. EXPERIMENTAL RESULTS

A. *s*-state anticrossings

In our initial report on anticrossing signals produced by blackbody radiation[9] we presented data for the avoided crossings of the s state with the lowest-energy linear Stark manifold state for several values of the principal quantum number n. Our new data have improved resolution and cover a wider range of n. We have also measured the avoided crossings of the s state with the second-lowest Stark manifold state for a subrange of these n values. The linear manifold level with lowest energy has $l=3$ in zero electric field, and we will therefore label this level with the parabolic quantum number[14] $n_1=3$. The manifold level with second-lowest energy has $n_1=4$, and so on.

A scan of the avoided crossing of the $20s$ state with the $n=18$, $n_1=3$ manifold state is shown in Fig. 3. The horizontal scale is obtained by converting the directly measured voltages to fields, using our 1.590(1)-cm plate separation. The presence of two peaks with unequal widths is explained in Fig. 4, where we show the energy levels involved in an avoided crossing of this type. We can see from this diagram that the left-hand peak in Fig. 3 corresponds to the $|m_l|=0$ component of the $n_1=3$ manifold state, and the right-hand peak the $|m_l|=1$ component. The quantum numbers $|m_l|$ are only approximate. When we include the fine-structure interaction only $|m_j|$ is a good magnetic quantum number, and the states which we have labeled $|m_l|$ contain small admixtures of other $|m_l|$ states. If the fine-structure interaction is not included the s state crosses the $|m_l|=1$ manifold state. Therefore the right-hand peak in Fig. 3 is

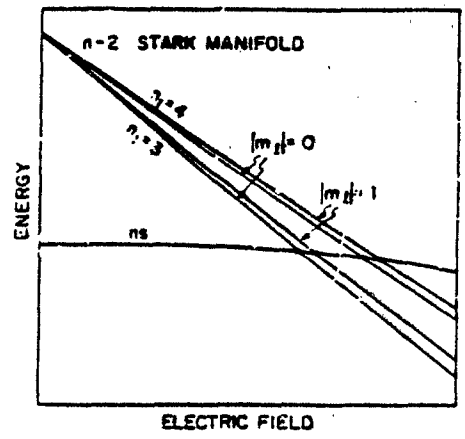

FIG. 4. Stark map for the avoided crossings of the ns state with the $n_1=3$ and $n_1=4$ states of the $n-2$ Stark manifold. The levels with higher n_1 are omitted for clarity. For each value of n_1 the nearly degenerate $|m_l|=0$ and $|m_l|=1$ levels are shown. For all levels shown $|m_j|=\frac{1}{2}$.

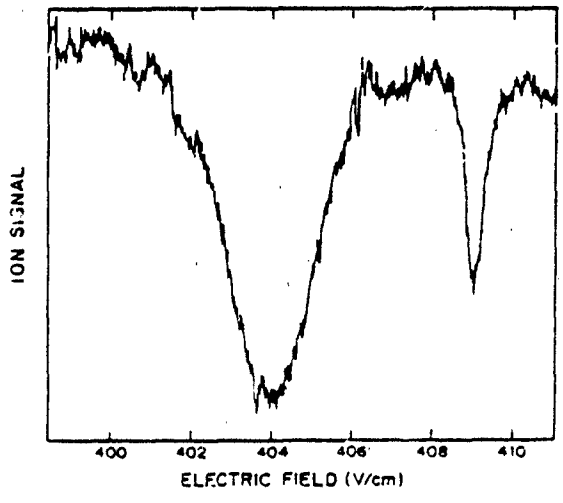

FIG. 3. Anticrossing signal from the avoided crossing of the $20s$ state with the $n=18$, $n_1=3$ Stark manifold state. The left-hand peak corresponds to the $|m_l|=0$ anticrossing, and the right-hand peak to the $|m_l|=1$ anticrossing.

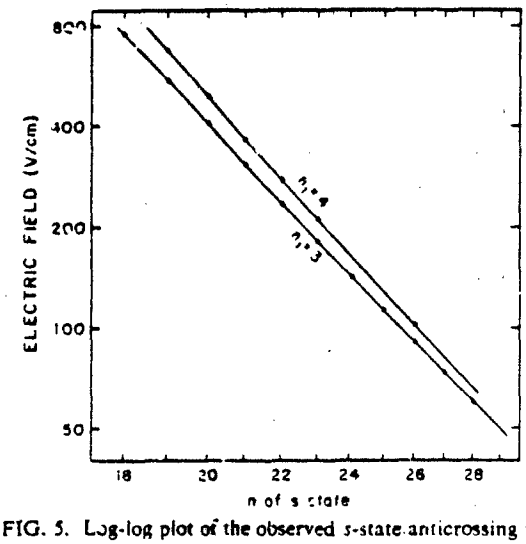

FIG. 5. Log-log plot of the observed s-state anticrossing field versus the effective quantum number n^*. Although the horizontal axis is labeled with the quantum number n of the s state, the scale is logarithmic in $n^*=n-\delta_s$. The lines are least-squares fits to the data.

TABLE I. Observed s-state anticrossing fields.

	$n_1=3$		$n_1=4$	
s state	$\lvert m_l\rvert=0$ (V/cm)	$\lvert m_l\rvert=1$ (V/cm)	$\lvert m_l\rvert=0$ (V/cm)	$\lvert m_l\rvert=1$ (V/cm)
18s	752.7(8)	763.5(7)		
19s	545.7(8)	553.1(5)	674.0(4)	684.0(5)
20s	403.9(5)	409.1(3)	491.1(13)	496.1(4)
21s	304.2(3)	307.9(2)	364.0(7)	367.6(3)
22s	232.7(2)	235.5(2)	275.0(4)	277.4(2)
23s	180.4(3)	182.6(2)	210.8(3)	212.6(2)
24s	141.8(2)	143.3(2)		
25s	112.5(1)	113.8(1)		
26s	90.25(6)	91.26(9)	102.7(1)	103.5(2)
27s	73.14(8)	73.90(8)		
28s	59.81(6)	60.44(5)		
29s	49.30(10)	49.78(7)		

due solely to the spin-orbit interaction. This accounts for its narrowness relative to the left-hand peak, which arises from the interaction between the Rydberg electron and the core.

The observed s-state avoided-crossing fields are given in Table I. In Fig. 5 we show a log-log plot of the s-state anticrossing field versus the effective quantum number n^* of the s state. Here $n^*=n-\delta_s$, where $\delta_s=2.18$ is the s state quantum defect. The points are the data and the lines are linear least-squares fits to the (log-log) data. Only the $\lvert m_l\rvert=0$ data are shown in the figure. The least-squares fits give the following results:

$$F=A(n^*)^P,$$

where

n_1	$\lvert m_l\rvert$	P
3	0	−5.20(1)
3	1	−5.21(1)
4	0	−5.45(2)
4	1	−5.48(2)

The exponents derived from the fits become more negative as we proceed into the manifold (i.e., as n_1 increases). We expect these exponents to be near −5 based on simple arguments. The Stark shifts [(energy)/(field)] of the manifold levels scale as $(n^*)^2$, and the zero-field energy spacing between the s state and the manifold states scales as $(n^*)^{-3}$. Therefore, if the relatively small Stark shift of the s state is ignored, the avoided crossing field is expected to scale as $(n^*)^{-5}$.

The observed widths of the s-state avoided crossings are given in Table II. In our previous report[9] the $\lvert m_l\rvert=1$ anticrossings were broadened by field inhomogeneity. The field plates used to obtain the present results have an estimated homogeneity of $\Delta F=1.0\times10^{-4}F$. A comparison with Table I shows that the widths given in Table II are not broadened by field inhomogeneity. The homogeneity was improved by using copper field plates[15] with larger area and smaller holes for ion extraction.

In Table III we compare our observed widths with theoretical widths obtained by diagonalization of the energy matrix.[8] The frequency widths are calculated directly, and are converted to field widths by using the conversion factors 356, 403, 450, and 506 MHz/(V/cm), for the 18–21s states, respectively. In all cases the observed widths are larger than the calculated widths. At least part

TABLE II. Observed widths for s-state anticrossings.

	$n_1=3$		$n_1=4$	
s state	$\lvert m_l\rvert=0$ (V/cm)	$\lvert m_l\rvert=1$ (V/cm)	$\lvert m_l\rvert=0$ (V/cm)	$\lvert m_l\rvert=1$ (V/cm)
18s	6.9(13)	0.63(6)		
19s	4.2(7)	0.50(6)	5.2(16)	1.0(4)
20s	2.3(2)	0.37(11)	7.5(19)	0.63(13)
21s	1.4(4)	0.23(6)	3.0(6)	0.39(9)
22s	0.9(2)	0.19(6)	1.9(3)	0.33(9)
23s	0.7(1)	0.13(6)	1.4(2)	0.28(6)
24s	0.7(2)	0.09(6)		
25s	0.6(3)	0.09(6)		
26s	0.27(6)	0.09(6)	0.38(6)	0.13(6)
27s	0.24(6)	0.09(6)		
28s	0.21(3)	0.06(3)		
29s	0.17(6)	0.08(4)		

TABLE III. Comparison of calculated and observed widths for s-state anticrossings ($n_1=3$).

	$\lvert m_l\rvert=0$			$\lvert m_l\rvert=1$		
s state	Calculated (MHz)	Calculated (V/cm)	Observed (V/cm)	Calculated (MHz)	Calculated (V/cm)	Observed (V/cm)
18s	930	5.2	6.9	80	0.45	0.63
19s	640	3.2	4.2	61	0.30	0.50
20s	450	2.0	2.3	47	0.21	0.37
21s	320	1.3	1.4	39	0.15	0.23

of this discrepancy appears to be due to the dispersion term in Eq. (12). For the $|m_l|=0$ anticrossings, the observed widths are 33, 31, 15, and 8% higher than the calculated widths for $n=18$–21, respectively. In fact our data do show progressively more asymmetric peaks for $|m_l|=0$ as we go from $n=21$ down to $n=18$.

B. p-state anticrossings

The p state also crosses the linear Stark manifold levels in potassium. In Fig. 6 we show a scan of one of these anticrossings, involving the 20p state and the $n=18$, $n_2=1$ manifold state (the manifold states are labeled, in order of decreasing energy, with the parabolic quantum number[14] $n_2=0,1,2,\ldots$). Figure 7 shows the energy levels involved in an avoided crossing of this type. Only $|m_j|=\frac{1}{2}$ levels are shown, and only the highest-energy manifold level ($n_2=0$) is shown (for both $|m_l|=1$ and $|m_l|=2$). The fine-structure interaction mixes a small amount of $|m_l|=1$ into the nominal $|m_l|=2$ manifold state. Therefore we have a situation similar to that of the s-state anticrossings. The anticrossing between the p state ($|m_l|=0$ and 1) and the $|m_l|=2$ manifold state (the peak at the right in Fig. 6) is due solely to fine structure and is consequently narrow, while the anticrossing involving the $|m_l|=1$ manifold state (the peak at the left in Fig. 6) is due to the core interaction and is much broader.

We have chosen laser polarizations which allow us to selectively populate the $|m_j|=\frac{1}{2}$ levels. The red laser is tuned to the $4s\rightarrow 4p_{3/2}$ transition, and is linearly polarized perpendicular to the electric field. This creates a 3:1 ratio of $|m_j|=\frac{3}{2}$ to $|m_j|=\frac{1}{2}$ population in the $4p_{3/2}$ state. The blue laser is linearly polarized parallel to the electric field, creating a preponderance of $|m_j|=\frac{1}{2}$ Rydberg states.

The observed p state $|m_j|=\frac{1}{2}$ anticrossing fields are given in Table IV. In Fig. 8 we show a log-log plot of the p-state anticrossing field versus the effective quantum number n^* of the p state. The points are the data and the lines are linear least-squares fits to the (log-log) data. The least-squares fits give the following results:

$$F=A(n^*)^P,$$

where

n_2	$\lvert m_l\rvert$	P
0	1	−5.18(1)
0	2	−5.21(1)
1	1	−5.30(1)
1	2	−5.35(1)
2	1	−5.48(1)
2	2	−5.53(1)

The exponents are again near −5, as they were for the s-state anticrossings. This is not surprising, since the scal-

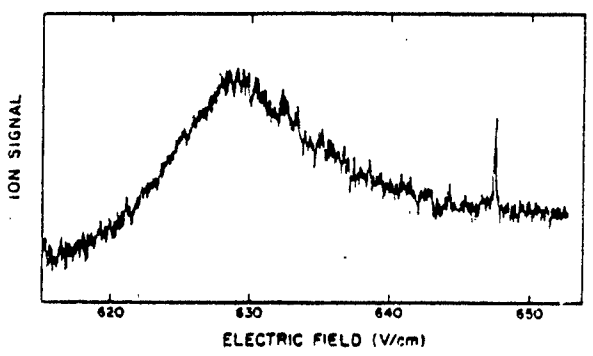

FIG. 6. Anticrossing signal from the avoided crossing of the 20p state with the $n=18$, $n_2=1$ Stark manifold state. The broad peak at the left is the $|m_l|=1$ anticrossing, and the narrow peak at the right is the $|m_l|=2$ anticrossing.

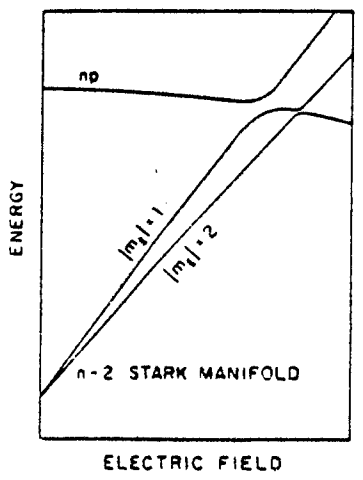

FIG. 7. Stark map for the avoided crossing of the np state with the $n_2=0$ state of the $n-2$ Stark manifold. The levels with higher n_2 are omitted for clarity. For all levels shown $|m_j|=\frac{1}{2}$.

TABLE IV. Observed p-state anticrossing fields.

p state	$n_2=0$ $\lvert m_l\rvert=1$ (V/cm)	$n_2=0$ $\lvert m_l\rvert=2$ (V/cm)	$n_2=1$ $\lvert m_l\rvert=1$ (V/cm)	$n_2=1$ $\lvert m_l\rvert=2$ (V/cm)	$n_2=2$ $\lvert m_l\rvert=1$ (V/cm)	$n_2=2$ $\lvert m_l\rvert=2$ (V/cm)
19p	737.7(13)	765.9(5)				
20p	551.8(16)	571.1(4)	627.6(8)	647.5(5)	725(3)	742.9(5)
21p	418.1(9)	432.6(3)	473.7(13)	486.7(3)	542(2)	553.4(4)
22p	321.7(7)	332.9(2)	362.0(10)	371.8(2)	410(2)	
23p	251.3(5)		280.6(7)		316(1)	

ing arguments given in the previous section for the s state apply equally well to the p states. Also, the p-state exponents become more negative as we proceed into the manifold (i.e., as n_2 increases), as did the s-state exponents.

The observed widths of the p-state $|m_j|=\frac{3}{2}$ avoided crossings are given in Table V. The $|m_l|=1$ widths vary considerably with n, while the $|m_l|=2$ widths remain relatively constant. Therefore it is safe to assume that the $|m_l|=2$ widths are limited by electric field inhomogeneity. Thus we obtain our estimate of $\Delta F=1.0\times10^{-4}F$ for the field homogeneity.

We have also observed the $|m_j|=\frac{1}{2}$ p-state anticrossings. We populate the $|m_j|=\frac{1}{2}$ Rydberg states by polarizing both lasers parallel to the electric field. In contrast to the p-state $|m_j|=\frac{3}{2}$ case, we do not observe narrow avoided crossing signals for $|m_j|=\frac{1}{2}$. This can be explained as follows. For $|m_j|=\frac{1}{2}$, there are two manifold states ($|m_l|=0$ and 1) for each value of n_2, and two p states (nominally $j=\frac{1}{2}$ and $\frac{3}{2}$). Both $|m_j|=\frac{1}{2}$ p states contain appreciable admixtures of both $|m_l|=0$ and 1. Therefore all four of the $|m_j|=\frac{1}{2}$ avoided crossings are due to core penetration and polarization. As a result these avoided crossings are relatively large. In contrast to the $|m_j|=\frac{3}{2}$ case, there are no $|m_j|=\frac{1}{2}$ avoided crossings which are due to fine structure alone. In fact the core interactions are so large that they produce a pair of "double" avoided crossings instead of four individual ones. This situation is shown in Fig. 9. As one might expect from Fig. 9, the anticrossing signals which we observe for $|m_j|=\frac{1}{2}$ are relatively complex, since each avoided crossing involves all four unperturbed levels.

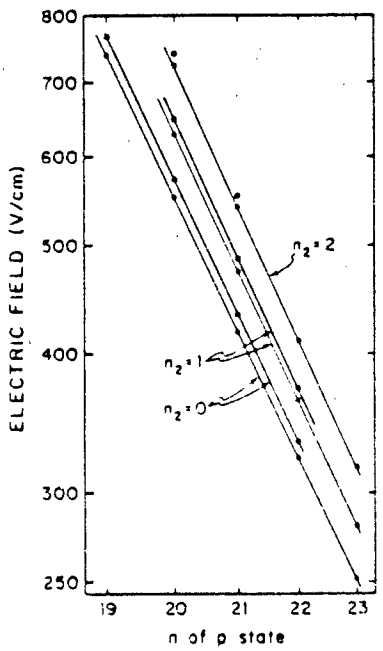

FIG. 8. Log-log plot of the observed p-state anticrossing field versus n. The lines are least-squares fits to the data.

C. Alternative experimental methods

In the course of these investigations we explored alternative schemes for the study of the avoided level crossings. The first is the obvious technique of examining the field ionization of the directly excited atoms. This signal is stronger than the blackbody signal, especially if the ionization pulse delay is reduced. The essential idea is shown in Fig. 10 for the specific case in which the excitation is primarily to the bold level. If the subsequent field ionization pulse leads to adiabatic ionization, then as the static field is swept through the crossing the ionization will

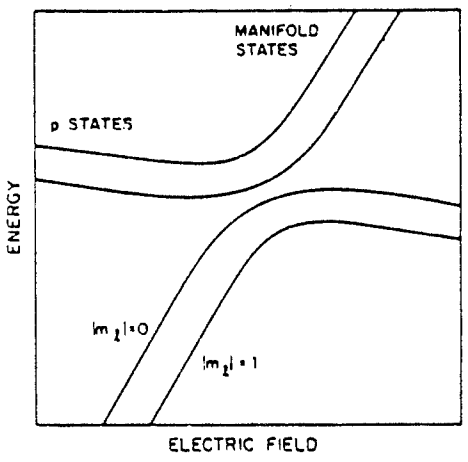

FIG. 9. Stark map for the avoided crossings of the fine structure p states with the $|m_l|=0$ and 1 manifold states, for $|m_j|=\frac{1}{2}$.

TABLE V. Observed widths for p-state anticrossings.

	$n_2=0$		$n_2=1$		$n_2=2$	
p state	$\lvert m_l\rvert=1$ (V/cm)	$\lvert m_l\rvert=2$ (V/cm)	$\lvert m_l\rvert=1$ (V/cm)	$\lvert m_l\rvert=2$ (V/cm)	$\lvert m_l\rvert=1$ (V/cm)	$\lvert m_l\rvert=2$ (V/cm)
19p	11(1)	0.06(3)				
20p	6.5(16)	0.08(5)	12(2)	0.11(3)	19(3)	0.09(3)
21p	5.2(8)	0.05(3)	8.7(13)	0.08(3)	11(2)	0.09(3)
22p	4.0(6)	0.06(3)	5.6(6)	0.05(3)	11(2)	
23p	2.6(4)		3.6(6)		8(1)	

change from occuring a point 2 to point 1. Thus if we detect ionization at point 2 (1) we would expect to observe a negative (positive) step. In practice this simple picture does not completely describe our observations. Two scans of the first s-state avoided crossing for $n=24$ are shown in Fig. 11. The laser excitation is primarily to the s state, which corresponds to the bold level in Fig. 10. The upper (lower) trace in Fig. 11 is for ionization occuring at point 2 (1) in Fig. 10. According to the above description we would expect each trace to show two steps corresponding to the $\lvert m_l\rvert=0$ and 1 avoided crossings. In fact we observe two steps with a sharp dip between them. This dip probably results from the dynamics of the field ionization pulse, preventing us from obtaining with confidence quantitative results from these direct measurements. This method does, however, provide a relatively easy way to find the approximate positions of the avoided crossings.

The second alternative method involves superradiant emission from the Rydberg state.[16] When the number of s-state Rydberg atoms is particularly high we observe an additional peak in the time-resolved field ionization signal. This peak occurs later than the normal signal, indicating that it originates from a lower-lying state. The size of the peak has a nonlinear dependence on the blue laser power. The peak disappears when we scan the dc voltage through an avoided crossing. When this noisy signal is present we also observe that the field ionization signal due to blackbody excitation to a higher state increases as we scan through an avoided crossing. Figure 12 shows an example of this effect for 20s. These observations can be explained by superradiant emission from the directly excited s state to a lower p state. This lower p state ionizes at a higher field and accounts for the extra peak in the time-resolved signal. As the dc voltage is scanned through the avoided crossing, the superradince is destroyed due to the mixing of states. The laser excitation into the s state is partially diverted into the manifold. Therefore at the avoided crossing fewer atoms are lost to

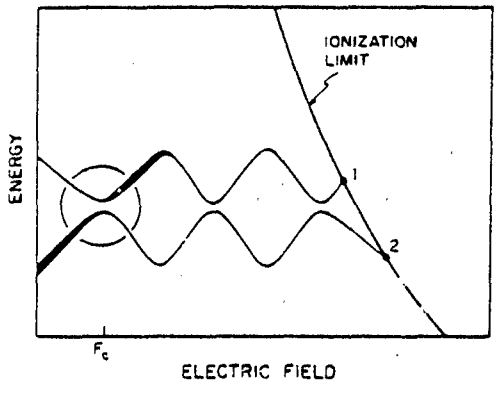

FIG. 10. Energy-level diagram for direct observation of anticrossings. The laser excitation to the circled avoided crossing is primarily to the bold level. Assuming adiabatic passage to the ionization limit, excitation with $F<F_c$ ($F>F_c$) leads to ionization at point 2 (1).

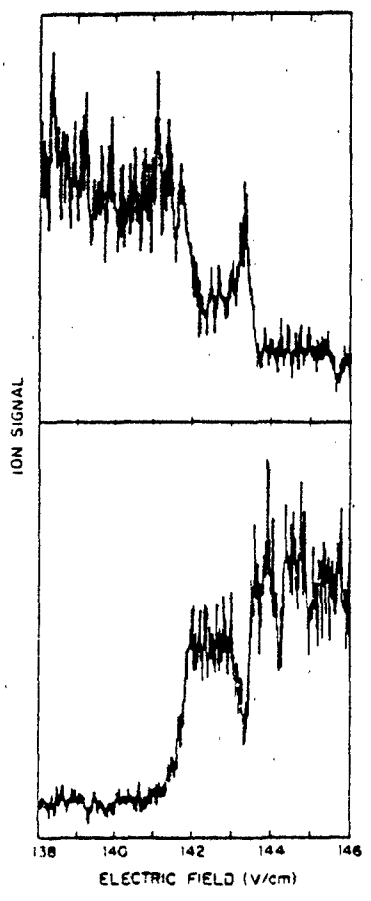

FIG 11. Direct anticrossing signals for 24s.

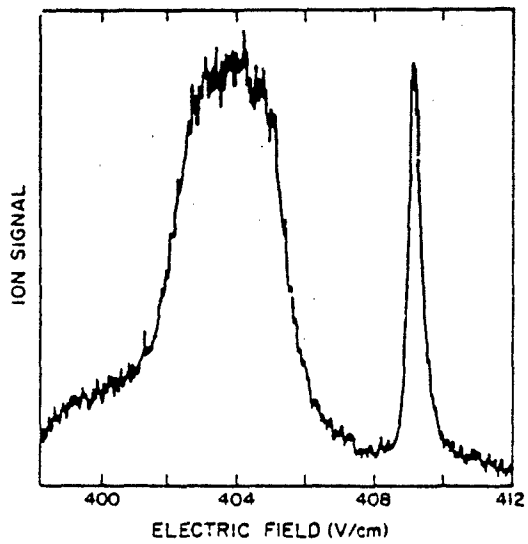

FIG. 12. Blackbody signal induced by superradiance for 20s.

superradiance, more are available for blackbody excitation, and the blackbody signal increases.

Although somewhat interesting in itself, the superradiant signal has limited quantitative usefulness due to the nonlinear nature of the superradiant emission. This saturation is evident in Fig. 12. For this reason the superradiance tended to be a nuisance. However, by keeping the number of excited atoms down we reduced this problem to a negligible level.

D. Uncertainties

There are several sources of uncertainty in these experiments. The foremost is the measurement of the plate spacing, 1.590(1) cm, which limits the absolute accuracy of the anticrossing field measurements given in Tables I and IV to roughly one part in a thousand. On the other hand, the resolution $\Delta F/F=10^{-4}$, with an absolute minimum of 0.04 V/cm, is limited by a combination of the spatial inhomogeneities, the laser spot size, and electrical pickup. This instrumental resolution has not been removed from the observed widths in Tables II and V. In most cases it is far smaller than the observed widths. We note that the field homogeneity over a larger region than the intersection of the crossed laser beams limited our day-to-day reproducibility of the anticrossing fields due to laser pointing variations. These variations however were less than uncertainty in the measurement of the plate spacing.

We extracted the anticrossing fields and widths visually from X-Y recorder tracings assuming that the anticrossing signals were symmetric Lorentzian peaks. As we have already pointed out the theoretical shape is a sum of Lorentzian and dispersion curves so this straightforward procedure is clearly not always correct, although inspection of a typical scan such as Fig. 3 suggests that it should be a reasonable approximation.

To estimate the magnitude of the error introduced by our simple analysis procedure we performed least-square fits to scans which represented both the typical nearly symmetric anticrossing signals and the most asymmetric ones. An example of the latter is the broad $|m_l|=1$ feature of Fig. 6. Fitting the data of Fig. 6 to a Lorentzian plus a dispersion curve gives a ratio of Lorentzian to dispersion of 1.6:1. The center obtained from the fit occurs at a field lower than the apparent (assuming only a Lorentzian line) center by 15% of the width, and the width obtained is less than the apparent width by 6%.

In the more typical case of Fig. 3, the errors are much less severe. Fitting the broad $|m_l|=0$ feature to a Lorentzian plus a dispersion curve shows that the ratio of their amplitudes is greater than 10:1, that the fit center differs from the apparent center by 3% of the width, and that the fit width is less than 3% smaller than the apparent width. In all cases the errors introduced by our method of analysis are less than the other uncertainties in the data. The stated uncertainties in the tables include those due to the analysis.

In principle we should be able to calculate the ratio of Lorentzian to dispersion in our signals by using Eq. (12), with the f and g values given by the method of Ref. 8. In practice, however, there is uncertainty in identifying the final states excited by the blackbody radiation, due to the complexity of the field ionization of potassium. For example, the final state for the s-state anticrossings is in principle a p state, but several nearby manifold levels contain appreciable admixtures of p character. Since the field ionization is not selective enough to distinguish between the p state and the nearby levels we cannot calculate the g values.

V. CONCLUSION

We have demonstrated a new method of anticrossing spectroscopy using pulsed excitation and a combination of blackbody radiation and field ionization for detection. We have used this method to measure avoided crossings between Stark levels of highly-excited potassium atoms. This method is complementary to the purely laser spectroscopic method and is particularly useful where the width of the avoided crossing is less than the laser width.

ACKNOWLEDGMENT

This work was supported by the Air Force Office of Scientific Research under Grant No. AFOSR-85-0016.

[1]F. D. Colegrove, P. A. Franken, R. R. Lewis, and R. H. Sands, Phys. Rev. Lett. 3, 420 (1959).

[2]T. G. Eck, L. L Foldy, and H. Weider, Phys. Rev. Lett. 10, 239 (1963).

[3]K. C. Brog, T. G. Eck, and H. Wieder, Phys. Rev. 153, 91 (1967).

[4]W. Nagourney, W. Happer, and A. Lurio, Phys. Rev. A 17, 1394 (1978).

[5]P. Hannaford and G. W. Series, Phys. Rev. Lett. 48, 1326 (1982).
[6]J. R. Rubbmark, M. M. Kash, M. G. Littman, and D. Kleppner, Phys. Rev. A 23, 3107 (1981).
[7]H. B. Van Linden Van den Heuvell, R. Kachru, N. H. Tran, and T. F. Gallagher, Phys. Rev. Lett. 53, 1901 (1984).
[8]M. L. Zimmerman, M. G. Littman, M. M. Kash, and D. Kleppner, Phys. Rev. A 20, 2251 (1979).
[9]R. C. Stoneman, T. F. Gallagher, Phys. Rev. Lett. 55, 2567 (1985).
[10]W. E. Cooke and T. F. Gallagher, Phys. Rev. A 21, 588 (1980).
[11]S. Haroche, M. Gross, and M. P. Silverman, Phys. Rev. Lett. 33, 1063 (1974).
[12]T. F. Gallagher, L. M. Humphrey, W. E. Cooke, R. M. Hill, and S. A. Edelstein, Phys. Rev. A 16, 1098 (1977).
[13]T. F. Gallagher and W. E. Cooke, Phys. Rev. A 19, 694 (1979).
[14]L. D. Landau and E. M. Lifshitz, *Quantum Mechanics: Non-relativistic Theory*, 3rd ed. (Pergamon, New York, 1977), p. 130.
[15]T. W. Ducas, W. P. Spencer, A. G. Vaidyanathan, W. H. Hamilton, and D. Kleppner, Appl. Phys. Lett. 35, 382 (1979).
[16]M. Gross, P. Goy, C. Fabre, S. Haroche, and J. M. Raimond, Phys. Rev. Lett. 43, 343 (1979).

Field ionization of the n = 8-15 states of sodium

J.L. Dexter and T.F. Gallagher

Department of Physics
University of Virginia
Charlottesville, VA 22901

Abstract

We report the electric field ionization of the n = 8-15 levels of Na using field pulses of risetime ~ 1 μs. The passage from low to high field is adiabatic, and the fields required for $|m_\ell| = 0$, 1, and 2 states are $3.12(9) \times 10^8\ n_s^{-4}$ V/cm, $3.37(11) \times 10^8\ n_s^{-4}$ V/cm, and $3.68(21) \times 10^8\ n_s^{-4}$ V/cm. Here n_s is the effective quantum number in the ionizing field. These values are in agreement with those determined previously for higher lying states.

Because of its simplicity, efficiency and relatively high selectivity electric field ionization using pulses of ~1 μs risetime has become a very useful tool for the study of atomic Rydberg states.[1] As a rule it has only been applied to states within a few hundred wave numbers of the ionization limit. For lower lying states, n<15, other approaches such as fluoresence or photoionization are more commonly used.

Whether or not field ionization is useful for the study of lower lying states depends upon two factors, the technical difficulties inherent in producing the requisite high fields and whether or not the passage from low to high field occurs in a simple fashion as for states of higher principal quantum numbers. For example does the electron spin remain coupled to the orbit for lower n states? To address these questions we have undertaken measurements of the field ionization of the Na n = 8-15 states which we report here.

The experimental set up is described in detail elsewhere,[2] so only a sketch of it will be presented here. The vacuum chamber is held at a pressure of 10^{-6} torr. The atomic source produces an effusive beam with a density of 10^{8}-10^{10} atoms/cm^3 in the interaction region. The beams from two tunable dye lasers, pumped by a Nd-YAG laser, intersect the atomic beam between two field plates. The first laser is tuned to one of the resonance lines of sodium, $3s_{1/2}$-$3p_{1/2}$ or $3s_{1/2}$-$3p_{3/2}$, the second is used to drive the transition from the $3p_j$ state to a Rydberg level, ns, nd, or np (with the assistance of a DC field which is approximately 1% of the field necessary for

ionization). Approximately 400 ns. after the Rydberg level is populated, a high voltage pulse is applied to the lower plate that defines the interaction region. Ions produced by field ionization are extracted through a hole in the upper plate and detected with an electron multiplier. The signal is then captured with a gated integrator, and the resultant averaged signal is recorded on an X-Y plotter.

The substantial change required to produce the requisite 100 kV/cm fields is in field plates. The upper plate is a 5 x 8 cm aluminum plate, 6 mm thick, with a 6mm diameter hole drilled in its center. A 0.02 mm thick electroformed mesh with 0.02 mm hole spacing is glued over the bottom of the hole in the plate with a ring of epoxy 1.5 cm in diameter. The mesh was held flat against the plate with a 1.2 cm diameter clamp while the glue dried. The excess epoxy was then removed with a razor blade and all epoxy lightly coated with silver paint. The lower plate is a piece of aluminum 3 cm x 5 cm with a raised center area 1.25 cm x 1.25 cm whose sides were rounded to avoid high voltage breakdown. It is suspended from the upper plate by bakelite standoffs 8mm long, and the two plates are held together with nylon screws. The final separation of the plates is 0.2564(25) cm. To further restrict the possible volume from which we could collect ions, we inserted a bushing of 1.51 mm inner diameter in the 6 mm diameter hole in the top plate. In principle this arrangement should produce a field homogeneity better than 1% over a 1 mm cube centered between the plates. In fact the homogeneity is better than 0.2% as shown by Fig. 1.

The pulsing circuit consists of a commercial trigger transformer; maximum output +20 KV; rise time 0.5μsec; that is connected to the lower plate. With this arrangement the field strength necessary for $n \geq 10$ can be attained. To ionize states of $n<10$ we use a second pulsing circuit to produce the negative complement of the first pulse, and this negative pulse is applied to the upper plate. With the triggering synchronized to within 25 ns the field strength was essentially doubled, so that $n \geq 8$ could then be ionized. The pulse voltages were measured with a Tektronix P6015 high voltage probe to an accuracy of ±3%, which was the dominant uncertainty in the measurements.

The thresholds for ionization of the different states were taken by slowly scanning the voltage supplied to the pulsing circuit connected to the plates. Figure 1 shows typical scans for the $10d_{3/2}$ and $10d_{5/2}$ states which show two and three thresholds respectively. The $nd_{5/2}$ states have three thresholds, the $nd_{3/2}$ and $np_{3/2}$ states have two thresholds, and the $np_{1/2}$ and $ns_{1/2}$ states have only one. This is consistent with completely adiabatic passage from the low field to high field states. The threshold fields are thus assigned in precisely the manner described in Ref. 2 to the high field $|m_\ell|$ states and are listed in Table I. Here m_ℓ is the azimuthal orbital angular momentum quantum number.

Fig. 1 shows another interesting feature. At a field of 38 kV/cm, just above the $|m_\ell| = 0$ threshold, the $|m_\ell| = 0$ field

ionization signal disappears. This is a clear manifestation of the fact that the classical threshold field for ionization $E_c = 1/16n_s^4$ is only an approximation to the fact that above this field the interaction with rapidly ionizing states of higher principal quantum number leads to ionization. If there is a fairly weak and localized interaction with a rapidly decaying state, as observed by Littman et al[3], it is possible to have the nonmonotonic behavior exhibited in Fig. 1. We observed similar behavior for the Na 12d $|m_\ell| = 0$ threshold. Recently this phenomenon has been studied carefully both experimentally and theoretically in He by van de Water et al.[4]

The data of Table I are plotted in Fig. 2 with the data of Ref. 2 to show the continuity. The line corresponds to the classical ionization limit of an $|m_\ell| = 0$ state, $1/16n_s^4$, which can be simply derived from a classical description of an atom in an electric field. Here, as in Ref. 2, n_s is the effective quantum number of the atom when the Stark shift of the adiabatic passage to the ionizing field is taken into account. Explicitly it is defined by the energy W_s of the atom at the point that it ionizes relative to the zero field limit by $W_s = -1/2n_s^2$. For the Na s, p, and d states the appropriate values of n_s for $|m_\ell| = 0$ are adequately given by

$$\begin{aligned} &s: \quad n_s = n-3/2 \\ &p: \quad n_s = n-1/2-1/n \end{aligned} \tag{1}$$

$$d: \quad n_s = n-1/2+1/n \quad .$$

The origin of the 3/2 for the s state and the 1/2 for the p and d states is shown graphically and explained in Ref. 2. The small 1/n terms, which were used in plotting Fig. 13 of Ref. 2 but not explained in the text arise in the following way. For each n manifold there are n $|m_\ell| = 0$ states which we assume to be evenly spaced in the strong field region. Thus two adjacent $|m_\ell| = 0$ states of principal quantum number n differ in n_s by 1/n.

A $1/16n_s^4$ threshold field dependence implies that the fractional difference in the ionizing field, $\Delta E/E$, between two states which pass adiabatically to two adjacent strong field $|m_\ell| = 0$ states is obtained by differentiating and noting that $\Delta n_s \sim 1/n_s$. Thus

$$\Delta E/E = 4/n_s^2 \quad . \qquad (2)$$

For high n states the difference in ionizing fields is quite small, but the lower n data of Table I allow a test of Eq. (2). Upon the application of the field pulse the s and d states pass to adjacent strong field states (Recall that the energy ordering in low field is preserved in the passage to high field.), and thus the difference in their ionizing fields should be given by Eq. (2). In Fig. 3 we plot $\Delta E/E_{s-d}$, the fractional difference in the (n+1) and nd $|m_\ell| = 0$ threshold fields as well as the prediction of Eq. (2) vs. $4/n_s^2$. In our opinion the agreement is quite good showing the utility of this

model.

Fitting the data points of Table I to an n_s^{-4} dependence gives the following threshold behavior,

$$|m_\ell| = 0: \quad E = 3.12(9) \times 10^8 \, n_s^{-4} \quad V/cm$$

$$|m_\ell| = 1: \quad E = 3.37(11) \times 10^8 \, n_s^{-4} \quad V/cm \qquad (3)$$

$$|m_\ell| = 2: \quad E = 3.68(21) \times 10^8 \, n_s^{-4} \quad V/cm \quad .$$

The uncertainties given in Eq. (3) are the standard deviations of the fits. These measurements are in agreement with the previous measurements[2,5] to within the stated uncertainties of both measurements.[2,5] The origin of the $|m_\ell|$ dependence of Eq. (3) has been described previously.[2,6]

This work shows that the lower lying Na states are ionized by a pulsed field in the same fashion as are the higher lying n = 15-20 states i.e., the electron spin becomes uncoupled as the field rises and the passage to the high ionizing field is adiabatic with respect to $|m_\ell|$. Furthermore it shows that selective field ionization of these low lying states is straightforward and thus should be useful in a variety of experiments.

This work has been supported by the Air Force Office of Scientific Research under grant no. AFOSR-85-0016.

References

1. J.A.C. Gallas, G. Leuchs, H. Walther and H. Figger, Advances in Atomic and Molecular Physics, eds D. Bates and B. Bederson, Vol. 20 (Academic Press, New York, 1985).
2. T.F. Gallagher, L.M. Humphrey, W.E. Cooke, R.M. Hill and S.A. Edelstein, Phys. Rev. A 16, 1098 (1977).
3. M.G. Littman, M.L. Zimmermann, and D. Kleppner, Phys. Rev. Lett. 37, 486 (1976).
4. W. van de Water, D.R. Mariani, and P.M. Koch, Phys. Rev. A. 30, 2399 (1984).
5. J.L. Vialle and H.T. Duong, J. Phys. B: Atom. Molec. Phys. 12, 1407 (1979).
6. W.E. Cooke and T.F. Gallagher, Phys. Rev. A 17, 1226 (1978).

Table I

(uncertainties are ± 3%)

State	$\|m_\ell\| = 0$ (kV/cm)	$\|m_\ell\| = 1$ (kV/cm)	$\|m_\ell\| = 2$ (kV/cm)
9s	95.49		
10s	58.08		
11s	38.24		
12s	25.38		
13s	17.49		
14s	12.90		
15s	9.71		
10p	39.46	42.68	
11p	26.37	27.62	
12p	18.21	19.61	
13p	12.97	13.32	
14p	10.38	10.93	
15p	7.59	7.97	
8d	90.34	104.55	
9d	55.11	63.03	69.32
10d	36.88	40.52	47.04
11d	24.51	27.09	29.17
12d	17.00	18.29	20.79
13d	12.52	12.86	13.51
14d	9.52	9.90	10.38

Figure Captions

Fig. 1 Na 10d field ionization signals vs ionizing field amplitude $10d_{3/2}$ state (lower trace) showing the $|m_\ell|$ = 1 and 2 thresholds. $10d_{5/2}$ (upper trace) observed with lasers polarized perpendicular to a small static field to allow the population of the $|m_\ell|$ = 5/2 states. The $|m_\ell|$ = 0,1 and 2 thresholds are indicated by the arrows are evident. Note the decrease in $|m_\ell|$ = 0 signal at field of 38 kV/cm.

Fig. 2 Plot of observed ionizing fields for Na from n = 8-20 plotted vs n_s, the effective quantum number in the strong field. The line indicates the classical ionization threshold.

Fig. 3 Plot of $\Delta E/E_{s-d}$, the fractional difference in the thresholds fields of the (n+1)s and nd states plotted vs. $4/n_s^2$. The solid straight line is the prediction of Eq. 2.

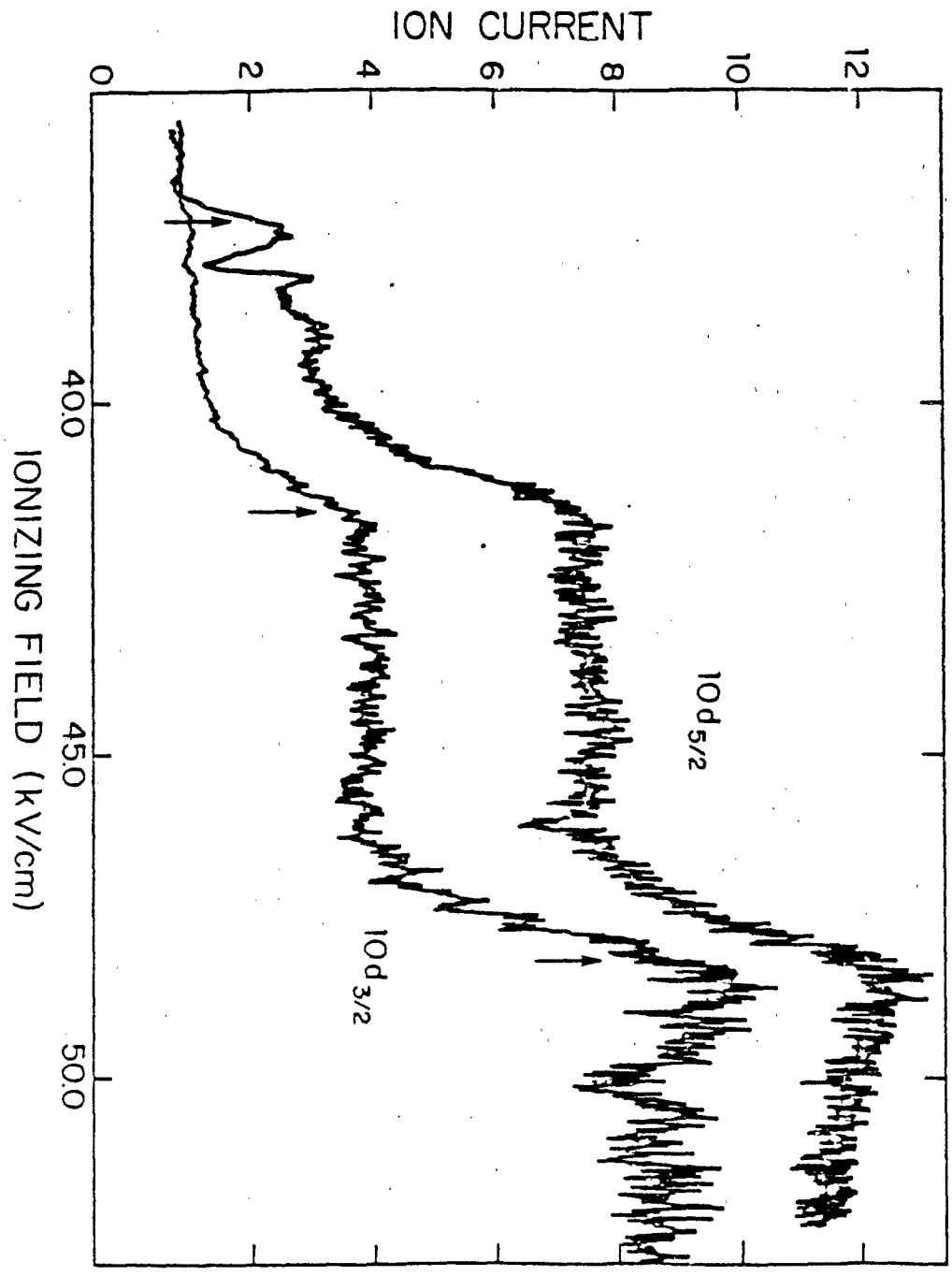
ION CURRENT
0
2
4
6
8
10
12
40.0
45.0
50.0
IONIZING FIELD (kV/cm)
10d5/2
10d3/2

Fig. 1

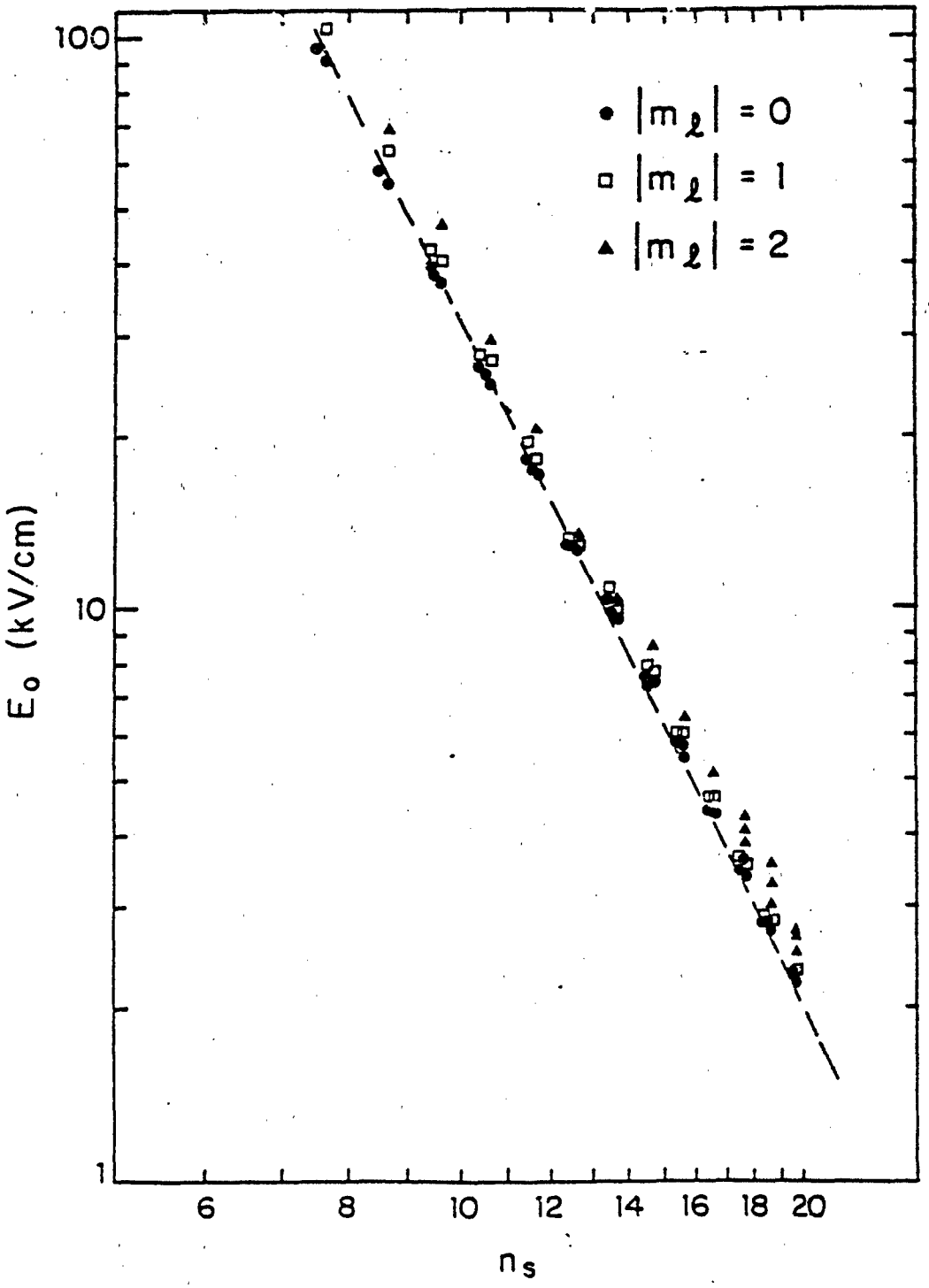

Fig. 2

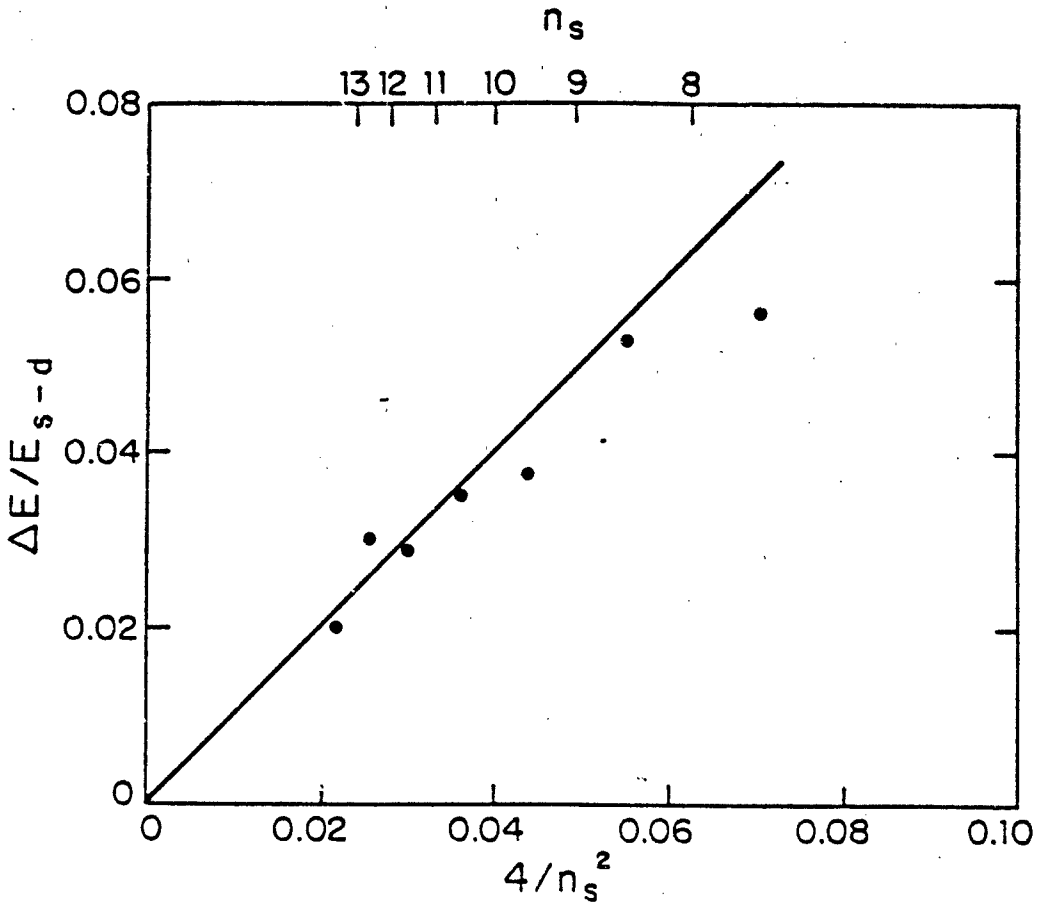
n_s
13 12 11 10 9 8
0.08
0.06
0.04
0.02
0
$\Delta E/E_{s-d}$
0
0.02
0.04
0.06
0.08
0.10
$4/n_s^2$

Fig. 3

Microwave Multiphoton Transitions Between Rydberg States of Potassium

L.A. Bloomfield, R.C. Stoneman, and T.F. Gallagher

Department of Physics

University of Virginia

Charlottesville, VA 22901

Received 14 March 1986

Abstract

We report the observation of sequences of one to as many as twenty eight photon transitions between potassium (n+2)s states and the lowest energy Stark states of the n manifolds for n=15-18. The sequences are observed by scanning a static electric field from the fields at which these pairs of levels nearly cross to zero field where they are well separated. The maximum number of photons absorbed is simply proportional to the microwave field.

The development of the laser has led quite naturally to the study and exploitation of highly nonlinear phenomena such as multiphoton excitation and ionization. For example the twenty-two photon ionization of He by 1.06μ light, scaling as $I^{21(2)}$ has been observed for I~ 5×10^{14}W/cm^2.[1] Not surprisingly, describing such highly nonlinear processes by a high order perturbation calculation is awkward and tedious. If, however, we express the above intensity as an electric field we see that it is ~4×10^8V/cm, a value comparable to the classical field required for ionization of a ground state He atom, 3×10^8V/cm^2. The similarity of the field strengths together with the inherently low frequency of the radiation used to drive multiphoton processes suggest that approaching the problem as the interaction of an atom with a strong time varying field might be profitable.

It has been appreciated for some time that one of the most quantitative ways of studying atoms in strong fields is to use Rydberg atoms, since the coulomb field experienced by the Rydberg electron is reduced by a factor of n^4, n being the principal quantum number.[3] For an n=20 atom only modest, easily characterized electric fields of ~2kV/cm are required to ionize the atoms. Furthermore recent experiments[4-6] with 8-15 GHz microwave fields have yielded results which differ dramatically from those obtained with static or quasistatic (~1MHz) fields. Specifically microwave field amplitudes of $1/3.7n^5$ (atomic units) were required to ionize a Na atom of principal quantum number n, in marked contrast to the static field requirement of $1/16n^{4}$.[4,6] The $1/3.7n^5$ field variation was attributed to the rate limiting step in the ionization process, a Landau-Zener transition from n to n+1 states which occurs at or near

the avoided crossing of the extreme blue shifted n Stark state with the extreme red shifted n+1 Stark state at a static field of $1/3n^5$. The transition occurs when an atom initially in level n is brought to the avoided crossing by the microwave field. If the field amplitude is enough to reach the avoided crossing and the size of the avoided crossing is roughly comparable to the microwave frequency the transition occurs, otherwise not.

While this simple Landau-Zener model seems to describe transitions driven by strong microwave fields, before one can comfortably apply such simple ideas to laser multiphoton problems, it seems imperative to observe the same microwave phenomenon in a form that clearly demonstrates the photon or quantized nature of the radiation. Some progress has been made in this direction by the observation of the quantized Floquet or sideband states produced by a microwave field.[7,8] As expected [9-11] the sidebands of a Stark state which has a linear Stark shift are observed to extend as far in frequency as the Stark shift produced by a static electric field of the same magnitude.[7,8] There is also in principle a decreasing tail of sidebands beyond this point which falls in amplitude by a factor of ten in two sidebands.[11] Thus the occurrence of the Na n→n+1 Landau-Zener transition has been shown to correspond to the overlap of the n and n+1 Floquet states when there is adequate coupling.[8] Still, the definitive experiment is the direct observation of multiphoton microwave resonances in these apparently field driven processes.

Here we report the observation of entire sequences of multiphoton microwave resonances in potassium. Specifically we have observed sequences of (n+2)s→(n,3) one to twenty-eight photon

transitions where (n,n_ℓ) denotes the Stark state of principal quantum number n which adiabatically continues back to the zero field $\ell=n_\ell$ state. Thus (n,3) indicates the lowest energy (m=0) member of the Stark manifold of principal quantum number n and it continues adiabatically to the zero field nf state. To our knowledge this is the first observation of such sequences of multiphoton transitions, and it completes the connection between the field and photon points of view.

The details of the atomic system are shown in Figure 1, a potassium level diagram near n=16 in a static field. As shown by Fig. 1 the $n=16,\ell>2$ states are nearly degenerate at zero field, so that in a field of >10V/cm they are better described as Stark states which have linear Stark shifts and therefore wavefunctions which are independent of the field. Only the two lowest (16,3) and (16,4) and the upper (16,15) Stark states are shown. The 18s state has virtually no Stark shift and is only weakly coupled to the n=16 Stark states, which are composed of $\ell>2$ states. The weak coupling is evidenced by the small size, 0.9 GHz, of the avoided crossing at 753 V/cm between the 18s and (16,3) levels.[12] The 16d state has a second order Stark shift due primarily to its dipole coupling to the 16f components of the n=16 Stark states. The sequence of transitions we have observed, $18s + q h\nu \rightarrow (16,3)$ for $1 \leq q \leq 28$ is shown schematically in Fig. 1.

Our experimental approach is shown in Figure 2. K atoms from an effusive source enter a microwave cavity through a 1.3mm diameter hole in the cavity sidewall. The atoms are excited from the ground 4s state to the 4p state to the 19s state by two 5ns pulsed dye laser beams entering the cavity through a 1.3mm diameter hole in the

opposite sidewall. A 0.5μs pulse of microwave power at a frequency of 9.285, 10.353 or 11.535 GHz is used to drive the transitions. After 1μs a high voltage pulse is applied to the septum in the cavity, producing a field which ionizes the excited K atoms and expels these ions through a 1mm diameter hole in the top of the cavity to a particle multiplier. The signal from the multiplier is captured with a gate set to accept the ionization signal from atoms in the $(16,n_1)$ states, but not the 18s state. The experiment is done by sweeping the static voltage applied to the septum and recording the increase in the $(16,n_1)$ population as the 18s-$(16,n_1)$ resonances are encountered.

The microwave cavity is a piece of WR90 waveguide 20.32 cm long, closed at both ends, and containing a copper septum. The cavity has a Q of 2100 at 10.353 GHz and is driven by an Avantek 7872 YIG tuned oscillator, amplified by a Hughes 1277H or an Alfred 623A travelling wave tube amplifier with output powers of 20W and 1.3W respectively. With our experimental configuration, 1W of power produced a field of 228V/cm. We are able to determine the microwave fields with an uncertainty of ±10%, and the static field homogeneity is 1%.

A typical example of a sequence of transitions is shown in Fig. 3 for the 18s→(15,3) transitions. These are scans of the (16,3) signal as a function of static field for a sequence of values of microwave field. For high static field few photons are needed and thus low microwave power is required. As we progress to lower static fields more photons are needed to make the transitions and thus more microwave power is required. The progression of one, two...twenty eight photons is quite apparent. We also note that there is negligible AC Stark shift until the very highest microwave powers, at

which a slight shift to higher static field is observed. For transitions between a state with a linear Stark shift and one with almost no static Stark shift only small AC Stark shifts are to be expected.[9,10]

Further support of our identification of the transition as (n+2)s-(n,3) irrespective of the static field value is obtained by extrapolating to the zero field intervals given in Table I. The intervals are consistent with transitions to hydrogen-like states of quantum defect $<5\times10^{-4}$, a requirement for the final state's being a Stark state. It is interesting to note that the intervals are > 15 GHz too large to match the (n+2)s-nf intervals (the nf quantum defect is 0.009[13]).

At a given microwave field several multiphoton resonances appear with comparable strength. This is approximately what would be expected, based on the simplest Floquet description of the process in which several of the Floquet states most displaced from the original (16,3) level have comparable amplitudes.[9,11] The one and two photon transitions are observed with small, 3V/cm and 20V/cm, microwave fields, but beyond that point the maximum number of photons absorbed increases linearly with the microwave field. In the Floquet picture this two photon offset corresponds to the decreasing tail of sidebands mentioned earlier.

The incremental fields required to absorb one additional photon are given in Table I. They scale as n^{-2}, as does the inverse of the static Stark shift. From these scalings we can determine the microwave field needed to drive the resonance nearest zero static field (we do not have enough power to see the transitions near zero

static field in all cases). These fields, scaling as n^{-5}, are given in Table I along with the previously measured static field crossings of the (n+2)s and (n,3) states.[12] As shown by Table I these microwave fields are only 60% of the static fields of the (n+2)s-(n,3) avoided crossings. In this case, the K (n+2)s→(n,3) interaction is through the nd state, which introduces a nonlinear Stark effect into the problem. Preliminary calculations and laser excitation spectra in the presence of microwave fields show that the presence of the nd state slightly below the nℓ>2 states leads to the existence of Floquet or sideband states at energies below the lowest Stark state in a static field of the same magnitude. Furthermore the (n+2)s→(n,3) transition is observed to occur when the Floquet or sideband states reach the s state.

For any given microwave field the transitions cannot be observed below some value of static field, due to lack of microwave field. Above some value of static field other resonances, not part of the 18s→(16,3) series appear. At relatively high static fields and low microwave fields it is easy to identify the beginning of this congestion as the 18s→(16,4) series of transitions, but at high microwave fields the spectrum becomes effectively continuous above some static field, and an unambiguous assignment is impossible. Nevertheless the effectively continuous spectrum is simply due to the overlapping series of transitions to many (16,n_1) Stark states.

The onset of the effectively continuous spectrum corresponds to the threshold for non-resonantly driving the transition. If we set the static field to zero and increase the microwave field we find a threshold for the (n+2)s-(n,3) transition, in some cases exhibiting

structure reminiscent of that observed by Mariani et al. in He^5. The observed structure is simply related to the location of the resonances near zero static field and the AC Stark shifts. For example, at 10.353 GHz the 19s-(17,3) 25 photon resonance shifts through zero static field at a microwave field of ~450V/cm. Thus in zero static field the 19s-(17,3) transition occurs for microwave fields between 400 and 500V/cm and only again for microwave fields > 750V/cm, where the spectral congestion occurs. This is a field slightly higher than the 19s-(17,3) level crossing. At 9.285 GHz however there is no such well placed resonance and a microwave field of ~750V/cm is required.

Although the off resonance thresholds of ~750V/cm correspond to the 19s-(17,3) level crossing field and thus to the Landau-Zener prediction, they are apparently due to the overlapping of many transitions. This coincidence is due to the fact that, for microwave fields equal to or greater the (n+2)s-(n,3) crossing field, the Floquet states of many of the (n,n_1) Stark states have appreciable amplitudes near the (n+2)s state, allowing the many overlapping transitions. However, there is a more fundamental connection between the multiphoton resonance and Landau-Zener pictures. As was shown by Rubbmark et al.[14] for a similar case, when many cycles of the field are used the Landau Zener description goes smoothly over to the resonance description. Since the transition amplitude can build up over many coherent microwave cycles it is hardly surprizing that lower microwave fields are required to drive the resonant transitions. We note that in the Na n→n+1 transitions, rapid mixing of the n Stark levels presumably removes any possibility of coherence

over many microwave cycles, and the single cycle Landau Zener description applies. Not surprisingly, no clear resonances were observed in that case and a field equal to ~ 80% of the crossing field was required to drive the transitions. This is in marked contrast to the case at hand in which the K s states are not mixed with any other states before making the (n+2) s-(n,3) transitions, and clear resonances are observed. In any case it is clear that an understanding of the levels in a static field allows us to identify the relevant level crossings and thus predict the radiation fields required for multiphoton processes to within a factor of two. This suggests that the field point of view might be employed more generally, to laser multiphoton processes for example, to yield useful insights with minimal calculational effort.

It is a pleasure to acknowledge the generous loan of a travelling wave tube by J.R. Grymes of Sperry Corporation, helpful discussions with H.P.Kelly, and the support of the U.S. Air Force Office of Scientific Research, under Grant No AFOSR-85-0016.

References

References

1. A. L'Huillier, L.A. Lompre, G. Mainfray, and C. Manus, J. Phys. B 16, 1363 (1983).

2. H.A. Bethe and E.A. Salpeter, Quantum Mechanics of One and Two Electron Atoms, (Academic Press, New York 1957).

3. R.N. Il'in Atomic Physics 3 eds. S.J. Smith and G.K. Walters (Plenum Press, 1973).

4. P. Pillet, W.W. Smith, R.Kachru, N.H. Tran and T.F.Gallagher, Phys. Rev. Lett. 50, 1042 (1983).

5. D.R. Mariani, W. van de Water, P.M. Koch and T. Bergeman, Phys. Rev. Lett. 50, 1261 (1983).

6. H.B. van Linden van den Heuvell and T.F. Gallagher, Phys. Rev. A 32, 1945 (1985).

7. J.E. Bayfield, L.D. Gardner, Y.Z. Gulkok and S.D. Sharma, Phys. Rev. A 24, 138 (1981).

8. H.B. van Linden van den Heuvell,R. Kachru, N.H. Tran, and T.F. Gallagher, Phys. Rev. Lett. 53, 1901 (1984).

9. S.H. Autler and C.H. Townes, Phys. Rev. 100, 703 (1955).

10. J.H. Shirley Phys. Rev. 138, B979 (1965).

11. M. Abramowitz and I.A. Stegun, Handbook of Mathematical Functions, National Bureau of Standards Applied Mathematical Series No. 55 (U.S. G.P.O. Washington, D.C., 1964).

12. R.C. Stoneman and T.F. Gallagher, Phys. Rev. Lett. 55, 2567 (1985).

13. P. Risberg, Ark. Fysik 10, 583 (1956).

14. J.R. Rubbmark, M.M. Kash, M.G. Littman, and D. Kleppner, Phys. Rev. A 23, 3107 (1981).

Table I

Incremental Field photon absorbed, zero field intervals, microwave fields required for the resonances nearest zero static field, (n+2)s-(n,3) static anticrossing fields.

Transition	Field/ photon absorbed (V/cm)	Zero field interval (GHz)	Microwave field (V/cm)	Anti-crossing field (V/cm)
17s-(15,3)	23(2)	----	740(80)	1058[a]
18s-(16,3)	18(2)	295(2)	480(50)	753[b]
19s-(17,3)	17(2)	246(2)	378(40)	546[b]
20s-(18,3)	14(2)	226(2)	242(30)	404[b]

a extrapolated from ref. 12

b from ref. 12

Figure Captions

Figure 1 Relevant energy levels near the n=16 Stark manifold. The manifold levels are labeled (n,n_1), where n_1 is the parabolic quantum number. Only the lowest two and highest energy manifold states are shown. The laser excitation to the 18s state is shown by the long vertical arrow. The 18s→(16,3) multiphoton rf transitions are represented by the bold arrows. Note that these transitions are evenly spaced in static field, and that transitions requiring more photons occur at progressively lower fields. For clarity, the rf photon energy shown in the figure is approximately five times its actual energy.

Figure 2 Schematic diagram of the apparatus showing the atomic beam and microwave cavity.

Figure 3(a) 18s→(16,3) one to fourteen photon transitions observed as the static field is scanned from 350-750V/cm for the microwave fields indicated above each trace (3.4 and 190 V/cm). The regularity of the progression is quite apparent. Note the extra resonances in the 142V/cm microwave field trace. These are due to 18s→(16,4) transitions.

Figure 3(b) 18s→(16,3) fifteen to twenty eight photon transitions observed as the static field is scanned from 0 to 350 V/cm for microwave fields from 270 to 460 V/cm. Note the congestion of the 410 V/cm trace at static fields above ~ 200 V/cm, due to many

overlapping (18s→16,n_1) transitions.

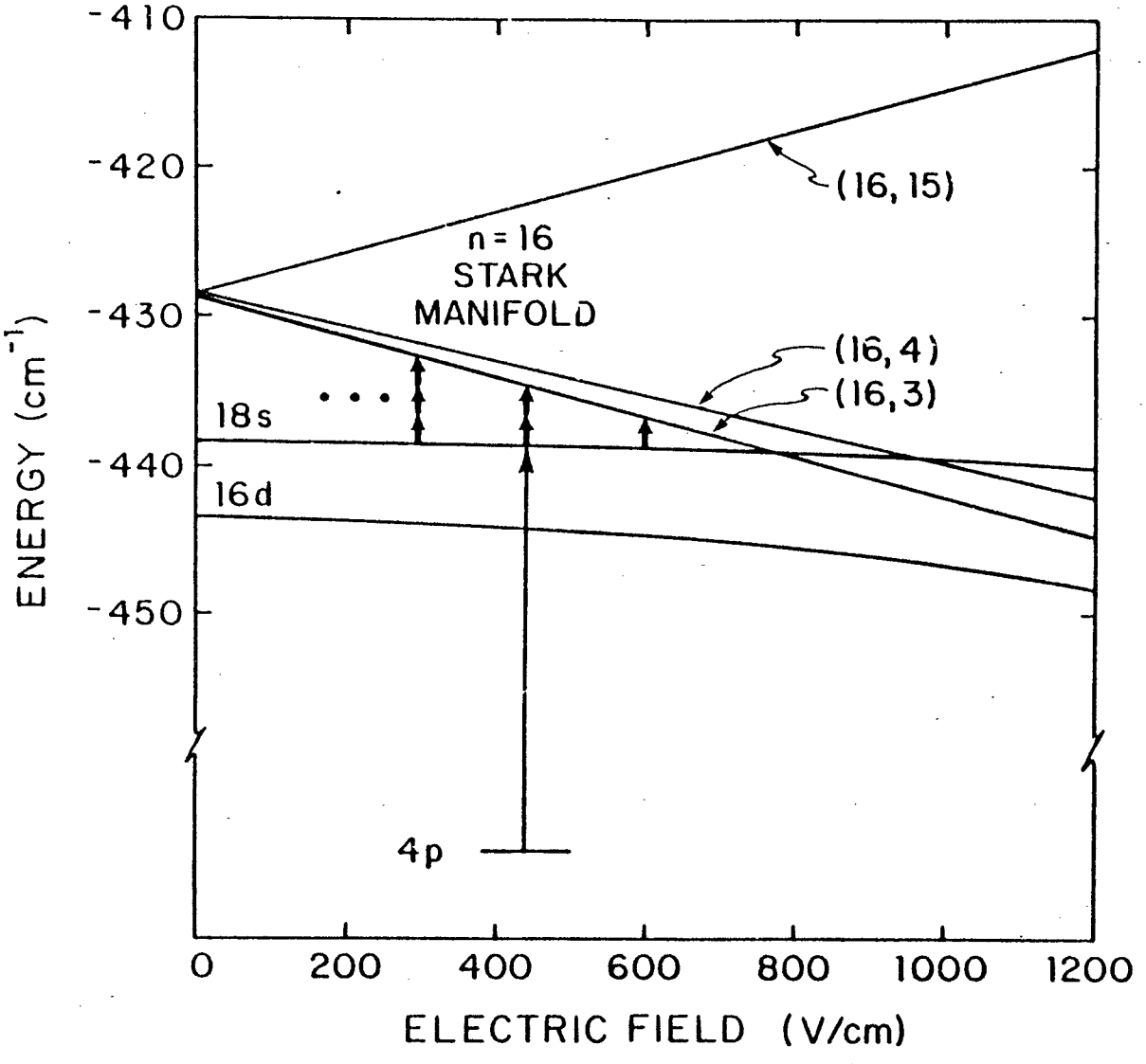
-410
-420
-430
-440
-450
ENERGY (cm^{-1})
(16, 15)
n = 16
STARK
MANIFOLD
(16, 4)
(16, 3)
18s
16d
4p
0
200
400
600
800
1000
1200
ELECTRIC FIELD (V/cm)

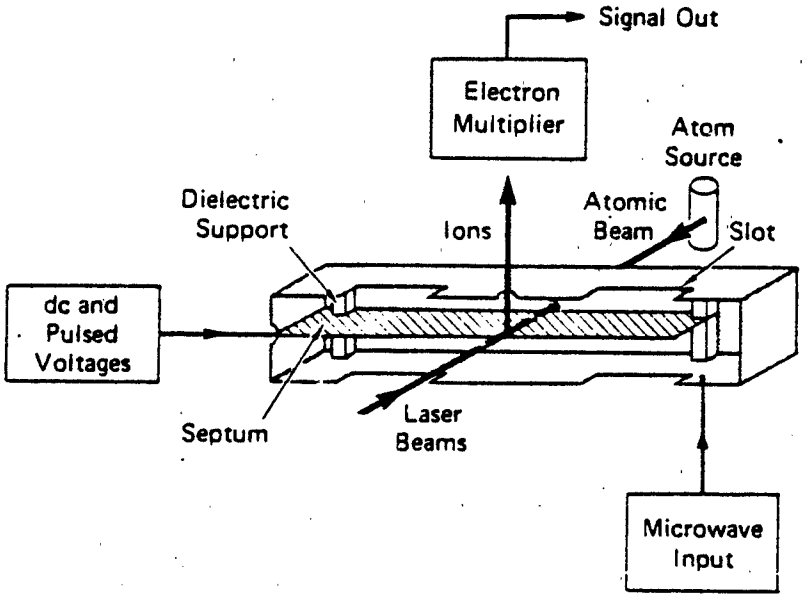
Signal Out
Electron Multiplier
Atom Source
Dielectric Support
Ions
Atomic Beam
Slot
dc and Pulsed Voltages
Septum
Laser Beams
Microwave Input

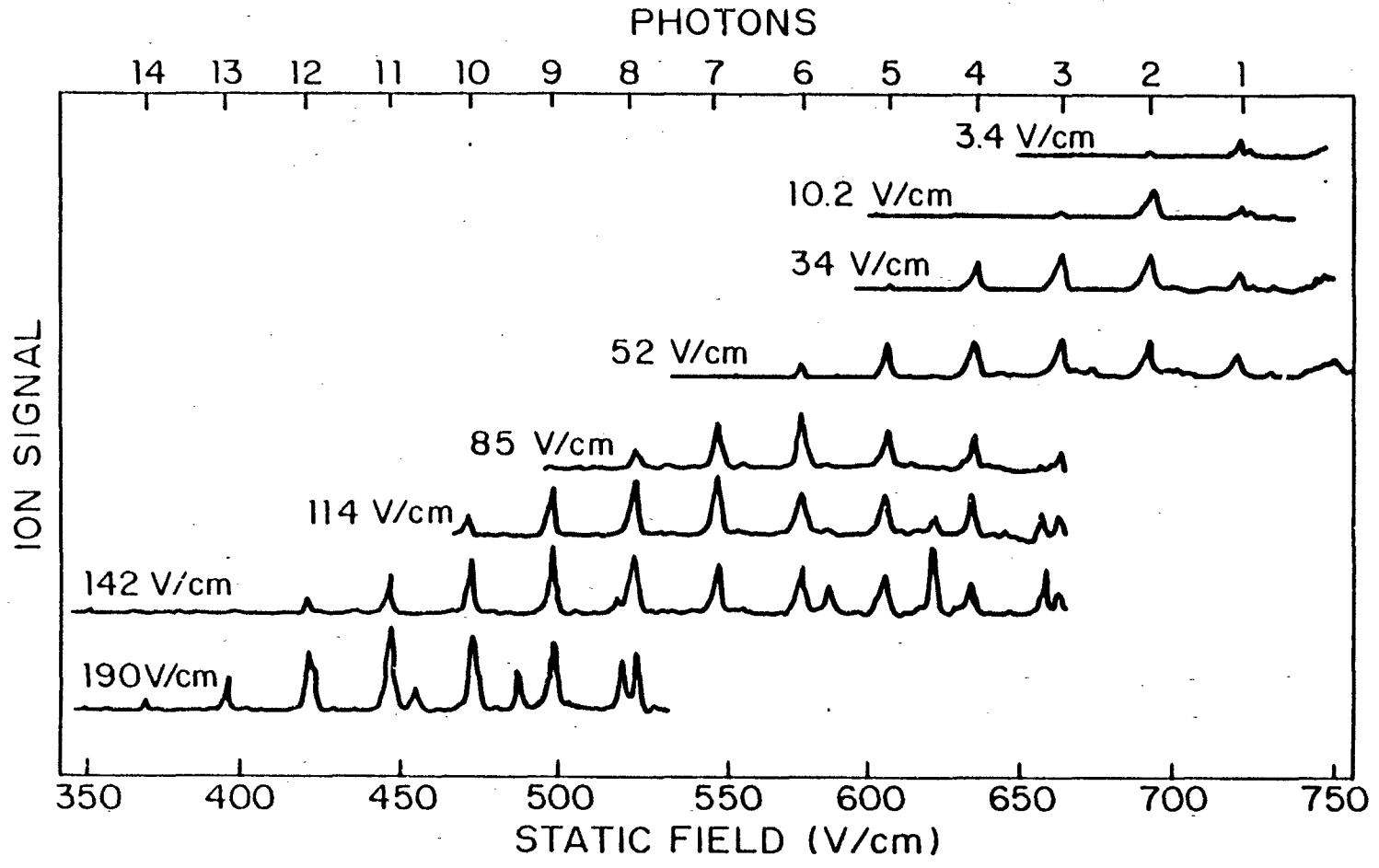
PHOTONS
14 13 12 11 10 9 8 7 6 5 4 3 2 1
3.4 V/cm
10.2 V/cm
34 V/cm
52 V/cm
85 V/cm
114 V/cm
142 V/cm
190V/cm
ION SIGNAL
350 400 450 500 550 600 650 700 750
STATIC FIELD (V/cm)

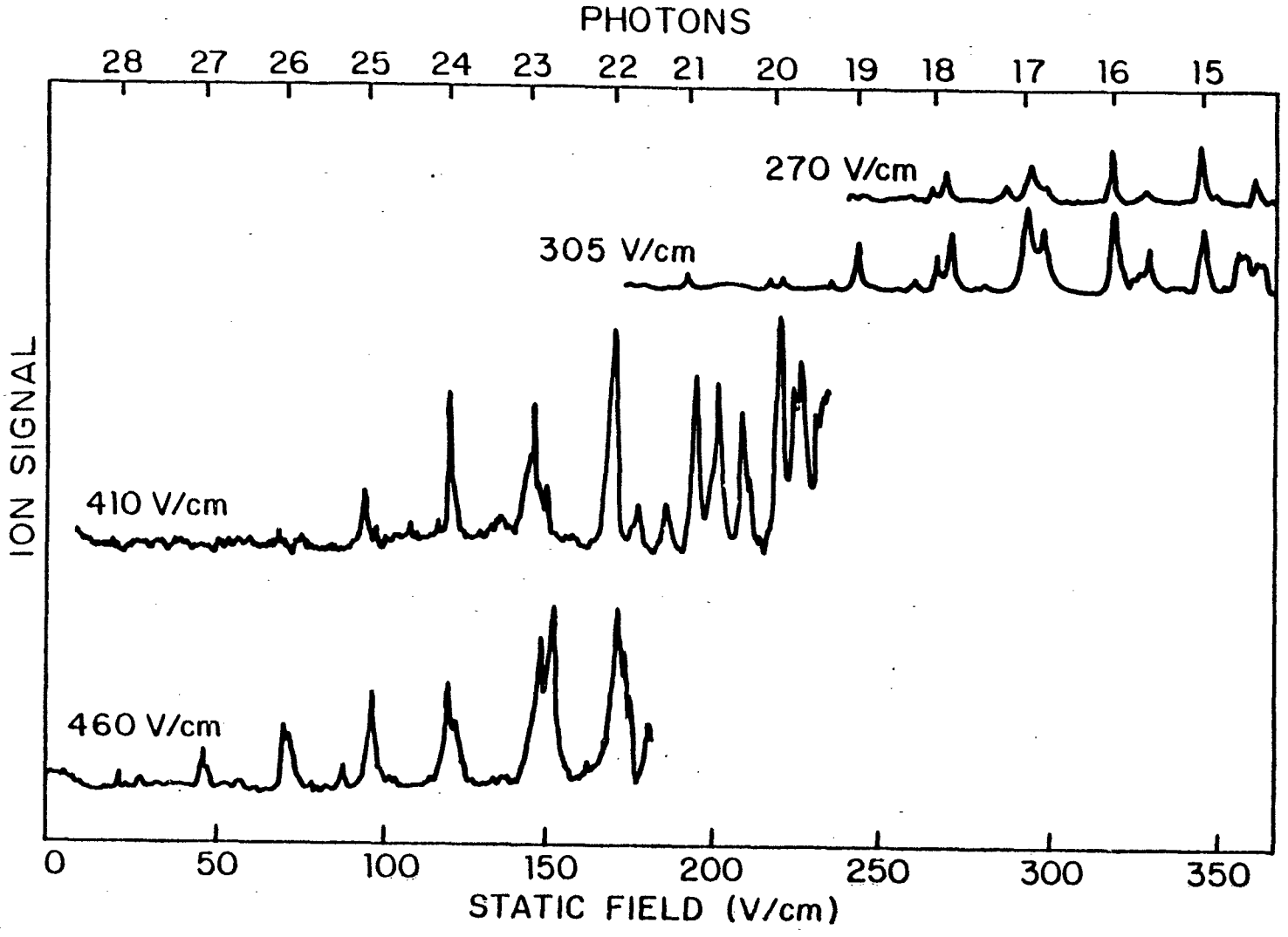
PHOTONS
28 27 26 25 24 23 22 21 20 19 18 17 16 15
270 V/cm
305 V/cm
410 V/cm
460 V/cm
ION SIGNAL
0 50 100 150 200 250 300 350
STATIC FIELD (V/cm)

Microwave Excitation and Ionization

T. F. Gallagher
Department of Physics
University of Virginia
Charlottesville, VA 22901

I. Introduction

Atoms may be ionized by static fields in excess of a threshold field $E = 1/16n^4$ where n is the principal quantum number [1]. On the other hand photoionization has a frequency threshold, requiring photons with energy in excess of the binding energy W. The rate of photoionization, though, is proportional to the intensity of the radiation, or E^2. Midway between these two processes is multiphoton ionization. Ionization by m photons requires that the photon energy be in excess of W/m, and in lowest order perturbation theory the ionization rate is proportional to I^m or E^{2m}. This scaling as I^m has been observed for m = 21, for higher values of m, or even for m = 21, it is difficult to measure an I^m dependence due to dynamic range considerations. Furthermcre, it is not clear that the region in which the lowest order solution is valid is physically very interesting, for appreciable ionization will only occur where it is not valid. In these cases it is more useful to describe the multiphoton processes as having field or intensity thresholds. Thus multiphoton ionization qualitatively resembles field ionization.

To generate a more solid understanding of the connection between photoionization and field ionization quantitative studies of the highly nonlinear multiphoton ionization process are required. One approach is to use tightly focused high powered pulsed lasers, and this has been done in the pioneering work at Saclay. However the spatial and temporal intensity variations inherent in the experiment make the study of highly nonlinear processes a challenge to say the least. Another approach is to use Rydberg atoms and microwave fields. As the microwave fields may be measured with a high degree of accuracy this approach allows very quantitative measurements to be carried out. This realization prompted Bayfield and Koch to begin the study of the microwave ionization of the Rydberg states of H [3].

Here we describe measurements of microwave excitation and ionization in alkali atoms. Alkali atoms, or any atom other than H, exhibit dynamical phenomena that can not be seen in H, under normal experimental conditions. For example in He, Na, K, and Ba the ionization by microwave fields requires a threshold field of $E = 1/3n^5$ [4-7].

II. Approach

The experimental approach [8] we use can be understood by inspecting Fig. 1. A thermal atomic beam passes into a microwave cavity through a hole in its sidewall, and the atoms in the cavity are excited by two pulsed dye laser beams entering through a hole in the opposite sidewall. For Na the lasers drive the transitions 3s → 3p and 3p → ns or nd. In the top of the cavity there is a small hole through which ions produced

can be extracted. The hole is located so that we only extract ions from an antinode of the microwave field ensuring the spatial homogeneity of the microwave field. As shown by Fig. 1 there is a septum in the cavity which allows the application of a static field to tune the atomic levels and extract ions produced by microwave ionization. A high voltage pulse may also be applied to the septum to selectively field ionize the excited atoms. We have used several microwave cavities at frequencies from 2-15 GHz of the general design shown in Fig. 1. These cavities have Q's in the range of 10^3 and allow us to produce fields of ~ 10^3 V/cm with 20W of input power.

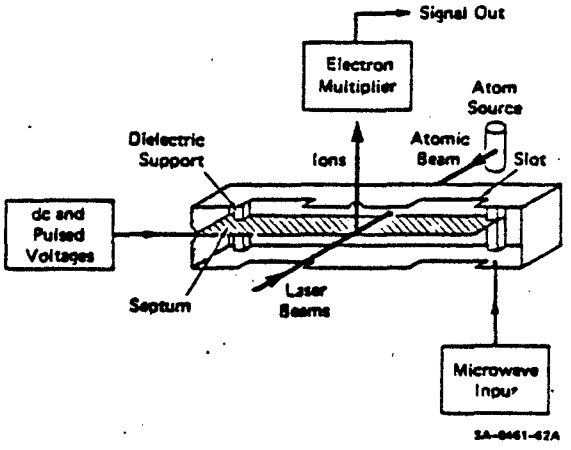

Fig. 1 View of the microwave cavity cut down the middle. Note that the laser and atomic beams enter on opposite sides of the cavity and the ions are extracted through the top.

With the apparatus shown in Fig. 1 it is possible to conduct a variety of investigations. Microwave ionization measurements are the most obvious, but the ability to do selective field ionization allows us to study as well microwave multiphoton transitions between levels.

III. Observations

The striking observation of an unexpected $1/3n^5$ threshold field for microwave ionization of Na by 15 GHz fields and similar results for He with 9 GHz fields showed that these atoms behaved very differently from H. The origin of this $1/3n^5$ dependence becomes clear upon examining Fig. 2, where we show how an initially excited Na 20d atom is ionized. The microwave pulse is applied to the cavity ~ 100 ns after the laser excitation, and in the filling time of the cavity, 100 ns, the atoms are redistributed over all the $n = 20$ $\ell \geq 2$ Stark states which are degenerate with 20d at zero field. Some, ~ 1/20 th, of the atoms are in the highest lying Stark state, and they move up and down in energy as the microwave field oscillates. If the field amplitude is sufficient to reach the point where the highest lying $n = 20$ Stark state intersects the lowest lying $n = 21$ Stark state the atom may undergo a Landau-Zener transition from one to the other at the avoided crossing of the levels shown in the inset of Fig. 2. The field at which this crossing occurs (for $m = 0$ states) is $1/3n^5$. Since the $n \rightarrow n+1$ crossing field becomes lower for higher n, once the atom has gone from $n = 20$ to $n = 21$ it can easily continue making such transitions and finally ionize.

Although it is possible for the Landau-Zener transition to occur, for it to be most likely the magnitude of the avoided crossing, ω_o, must be comparable to the microwave frequency ω [4,5,8]. Due to the large number of microwave cycles in any real experiment this requirement is

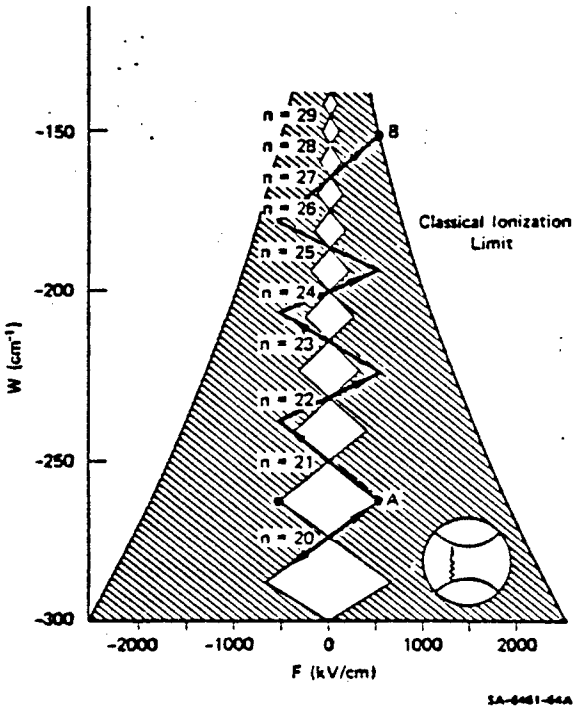

Fig. 2 Schematic diagram of the ionization of Na n=20 atoms by a 600 V/cm microwave field. Of the initially excited n=20 atoms some are in the highest energy Stark state and are brought to point A by the oscillating field as shown by the bold arrow. At point A the atoms can make a Landau-Zener transition to the lowest n=21 Stark state as shown by the inset. Further transitions to successively higher n states ensure culminating in ionization when it becomes classically allowed at point B.

rather loose. Nonetheless we note that with a microwave frequency of 15 GHz this form of ionization occurs for the Na $|m| = 0$ and 1 states, for which $\omega_o \sim 1\ cm^{-1}$ at $n = 20$. For the $|m| = 2$ states, which have $\omega_o \sim 0.01 cm^{-1}$, it does not occur. In fact for Na the Na $|m| = 0$ and 1 states, frequencies of 2-15 GHz are equally effective in producing the $1/3n^5$ ionization.

The $1/3n^5$ field is of course the field for the rate limiting $n \rightarrow n+1$ transition. The transitions from Na s and p states of non-zero quantum defect to nearby Stark manifolds also exhibit threshold fields in accord with this model. These are all transitions, presumably multiphoton, to real states, and one must ask if they can be observed in such a way as to clearly exhibit this character. Preliminary surveys in Na did not reveal this; however a more recent experiment with K has.

In Fig. 3 we show a K energy level diagram in an electric field. We have observed the transition from the 18s state to the n = 16 manifold. Specifically we have concentrated on the transitions to the lowest states of the manifold as shown by Fig. 3. In the experiment we populate the 18s state and observe the population transferred to the 16 manifold state using selective field ionization. The cavity fixes the microwave frequency, and we tune the atomic levels by sweeping the static field. As shown by Fig. 4 we see the series of 18s - lowest Stark state resonances, separated by 28 V/cm, corresponding to 1,2,3... photon transitions. For any given scan the congestion at higher static field is due to transitions to the numerous higher Stark states. For low microwave powers these are readily identified, but for higher powers the overlap is too severe. An analysis of the microwave field dependence shows that the one and two photon transitions occur for low microwave power, but beyond that point the number of photons absorbed

Begin text of second and succeeding pages here. DO NOT [illegible]

varies as E_{mw}, the microwave field amplitude. This is well out of the perturbative regime. However it is completely consistent with expectations based on the creation of sidebands of the Stark state by the microwave field [9-11].

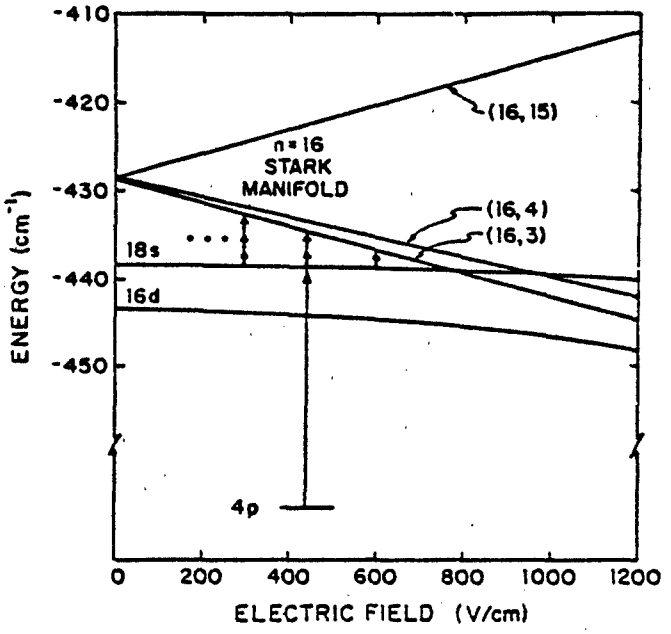

Fig. 3 K level diagram in an electric field. The 16s state is populated by the laser, and the entire sequence of microwave multiphoton transitions to the (16,3) Stark state is observed by selective field ionization of the (16,3 state. Transitions to higher Stark states such as (16,4) are also observed.

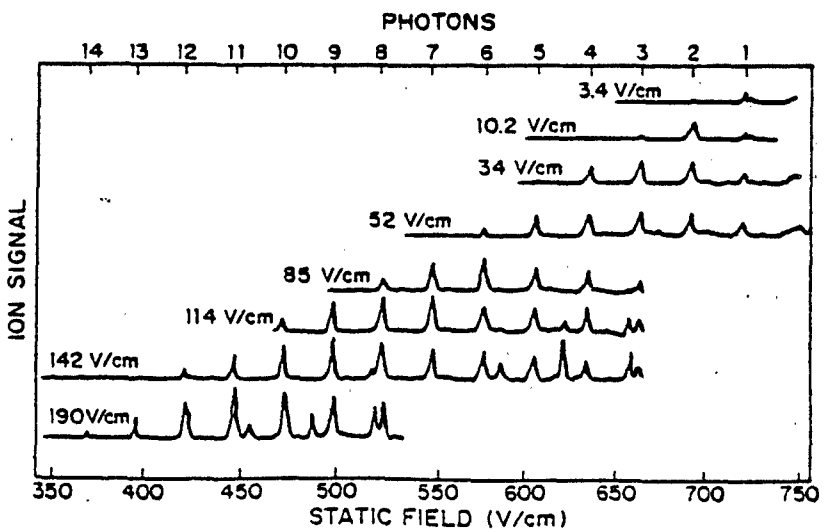

Fig. 4a Multiphoton 18s-(16,3) transitions observed by scanning the static field with a microwave frequency of 10.353 GHz and the microwave field amplitudes given by each trace. The resonances corresponding to the absorption of each additional photon are 28 V/cm apart. Note that for microwave fields of 114 V/cm, 142 V/cm and 190 V/cm that extra lines appear which are part of the analogous 18s-(16,4) series of resonances.

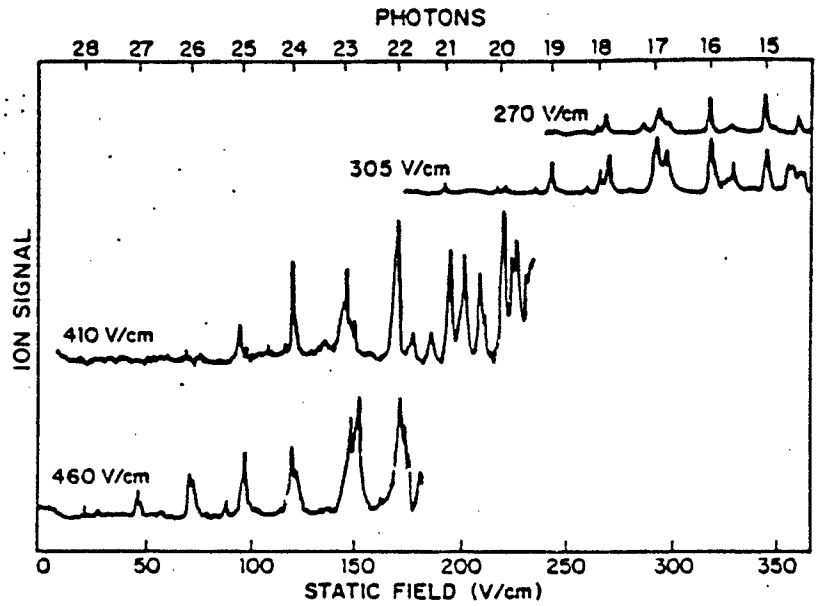

Fig. 4b Multiphoton 18s-(16,3) resonances at higher microwave fields than Fig. 4a, allowing zero static field to be reached. Note the spectral congestion in the trace for a microwave field of 410 V/cm. This is due to overlapping transitions to higher states of the n=16 Stark manifold.

To show the relation to the Landau-Zener model we have measured the threshold for the ns→(n-2) manifold transition as a function of the microwave field amplitude (with zero static field). The non-resonant microwave field required is ~ 800 V/cm, about 10% higher than the crossing field of 753 V/cm, in good agreement with the Landau Zener model. Note though that the resonance near zero static field only requires a microwave field of 460 V/cm, 60% of E_c. However if we examine the E_{mw} = 410 V/cm scan we see that the onset of serious overlap in the resonances occurs at E_s = 200 V/cm. This occurs at a lower static field for E_{mw} = 460 V/cm and finally occurs at zero static field for E_{mw} = 800 V/cm.

IV. Conclusion

At this point it is clear that the Landau-Zener picture is intimately related to a multiphoton resonance description. This is not really surprising as the resonance picture is simply a many cycle, coherent Landau-Zener picture. An aspect that is definitely unclear is the effect of other competing transitions on the observed resonances. For example the n = 16 manifold states are easily mixed by microwave fields of a few V/cm, yet the 18s - 16 manifold resonances are still very evident in Fig. 4. This and other questions are currently under study.

Acknowledgements

This represents the efforts of several people, among them P. Pillet, H.B. van Linden van den Heuvell, J.L. Dexter, L.A. Bloomfield and R.C. Stoneman. The research has been supported by the Air Force office of Scientific Research under grant AFOSR-85-0016.

References

1. F.B. Dunning, R.F. Stebbings: In Rydberg States of Atoms and Molecules; ed. by R.F. Stebbings, F.B. Dunning (Cambridge University Press, Cambridge, 1983) p. 315
2. A. L'Huillier, L.A. Lompre, G. Mainfray, C. Manus: J. Phys. B 16, 1363 (1983)
3. J.E. Bayfield, P.M. Koch: Phys. Rev. Lett.
4. P. Pillet, W.W. Smith, R. Kachru, N.H. Tran, T.F. Gallagher: Phys. Rev. Lett. 50, 1042 (1983)
5. D.R. Mariani, W. van de Water, P.M. Koch: Phys. Rev. Lett. 50, 1261 (1983)
6. L.A. Bloomfield, R.C. Stoneman, T.F. Gallagher: (unpublished)
7. U. Eichmann, J.L. Dexter, E.Y. Xu, T.F. Gallagher: (unpublished)
8. P. Pillet, H.B. van Linden van den Heuvell, W.W. Smith, R. Kachru, N.H. Tran, T.F. Gallagher: Phys. Rev. A 30, 280 (1984)
9. S.H. Autler, C.H. Townes: Phys., Rev. 100, 703 (1955)
10. J.H. Shirley: Phys. Rev. 138, B979 (1965)
11. J.E. Bayfield, L.D. Gardner, Y.Z. Gulkok, S.D. Sharma: Phys. Rev. A 24, 138 (1981)
    J.R. Rubbmark, M.M. Kash, M.G. Littman, D. Kleppner: Phys. Rev. A 23, 3107 (1981)

Text should end on this page